Author's final response

Trends of atmospheric water vapour in Switzerland from ground-based radiometry, FTIR and GNSS data

Bernet et al., Atmos. Chem. Phys. Discuss., 2020, https://doi.org/10.5194/acp-2020-77

Dear referees, dear editor Geraint Vaughan,

we would like to thank the referees for the constructive and elaborated comments and suggestions to our manuscript. We have taken the remarks into account and hope that we have responded satisfactorily to the suggestions. The referee's comments are given in blue italic typeface, our responses are given in black, and the corresponding changes in the manuscript in grey. Further, we attach a revised version of the manuscript with marked changes.

Kind regards,
Leonie Bernet (on behalf of all co-authors)

Contents

1 Author's response to referee #1

1.1 General comments

The paper is a detailed study of the IWV data (and trends) gathered by all available IWV measurement devices available in Switzerland, and extended with the most state-of-the-art reanalysis output available (ERA5 and MERRA-2). The use of a trend analysis model that account for possible biases (inhomogeneities) due to instrument changes is really a strong point of this study. At some places, the study does lack some interpretation of the findings (see my specific comments), and I identified three remaining caveats the study should deal with before publication:

Thank you for your feedback, we have followed your suggestions to improve the manuscript.

In the analysis of equations (9), (10), and (11), it is assumed that the relative humidity is constant, as is quite often the case when assessing the impact of the Claussius-Clapeyron relationship. However, in the study of Wang et al. (2016), already referred to in the manuscript, but not in this section, it is shown that the relative humidity varies with temperature. As you might have relative humidity measurements available (in any case you might use the reanalyses output), it would be good to confront your approach with the one described in Wang et al. (2016). In the conclusions section (lines 505-509), you also highlight this weakness in your approach. I think that adding the variation of relative humidity with temperature as an extra piece of information to understand the variation of IWV with temperature in Switzerland should be considered.

We thank the referee for this input and agree that analysing the variation in relative humidity can provide valuable information. We therefore added a figure showing RH trends from ERA5 (Fig. 15 in new manuscript). The text and interpretation were adapted accordingly.

Description of new Fig. 15:

ERA5 e_s is decreasing in winter, whereas ERA5 IWV winter trends are increasing. These conflicting results indicate that the assumption of constant relative humidity might not be valid in winter. This is confirmed by the ERA5 RH trends (Fig. 15), which are around zero for whole Switzerland in all seasons but slightly positive in winter. Even though these positive winter RH trends are not significantly different from zero, they raise the question whether it is justified to assume RH to be constant.

Conclusions:

Another reason for observed inconsistencies between temperature and IWV changes might be changes in relative humidity (RH). **Our temperature–IWV relation assumes that the relative humidity remains constant. However, we found positive RH trends in winter using lower tropospheric ERA5 data. Even though the RH trends are not significant, they might partly explain the disagreement between observed winter temperature and IWV changes. Wang et al. (2016) states that RH may not be constant because of limited moisture availability over land surfaces.** ~~However, this is not always the case, because of limited moisture availability over land surfaces (Wang et al. 2016)~~ Some studies found even a decrease of relative humidity with increasing temperature at midlatitudes (O'Gorman and Muller, 2010) or in the subtropics (Dessler et al., 2008). **Further analyses with additional data sets would be required to provide more insights into possible RH trends in Switzerland.**

Another major point I want to raise here, is the comparison of trends (especially in section 6.1) between GNSS sites that have a different length of time series. The length of the time series is only considered in the size of the markers in Fig. 8, but will interfere with other effects that have considered to compare the trends (e.g. the altitude of the station, in Fig. 9, to name only one). Due to the inter-annual variability of IWV, the starting/end date of the time period has an impact on the trend value. Therefore, I would urge for a detailed analysis of the impact of the length of the time series on the resulting IWV trends, by e.g. constructing an alternative Fig. 8 with trends calculated from a common time period and/or constructing a figure like Fig. 9, in which the trend is assessed against the starting year of the GNSS time series.

The length of the time series can indeed affect the trend and its uncertainty in multiple ways.
1. The longer the time series is, the more information is available. However, the information content of the data is often overestimated because the data might not be truly independent. Any variability in the data which is not accounted for by the trend model can lead to autocorrelations in the fit residuals. These are, however, taken into account by the trend analysis tool used. Even if the length of our time series appears to be short, the impact of this shortness and the information loss via autocorrelations is included in the uncertainty estimates provided.
2. Also, systematic short-term variability can mimic trends which are not there in the true atmosphere. For example, an unaccounted annual cycle will give rise to an artificial trend if the length of the time series is different from an integer multiple of a full year. However, the trend model we use includes the annual cycle and three of its overtones. Thus, these effects should not cause any artefact.
3. Another possible cause of the dependence of the trend from the start and end date of the time series might be that the trend is not linear. Since our trend model assumes a linear trend, our resulting trends might indeed depend on the start and end date of the time series. We therefore indicate the length of the time series in Table 1 and show the different lengths by the marker size in Figure 8. To make these different trend lengths also visible in the altitude dependent Figure (Fig. 10 in new manuscript), we added trend length dependent marker sizes also in this figure. Further, we added GNSS trends to the reanalysis maps (Figures 11 and 12 in new manuscript), showing only GNSS trends with longest time series (18 and 19 years). Finally we would like to mention that Fig. 8 (Fig. 9 in new manuscript) shows for the majority of the Swiss GNSS stations positive trends of IWV in spite of different start and end times of the IWV series. This is also an important result of our study.

The section 4.1.1 is definitely not my favorite section. It leans on Fig. 5, in which the trend uncertainty bars should be added. This might be tricky, since, as far as I understand, those monthly trends were computed based on only one value a year, so based on about 20 points (20 years) only. Besides this small amount of points, the length of the time series is very short in climatological sense (where time periods of 30 years are the standard). As a matter of fact, there are some interesting studies that calculate the number of years that is needed to derive a statistically significant trend in IWV (e.g. Alshawaf, F., Zus, F., Balidakis, K., Deng, Z., Hoseini, M., Dick, G., and Wickert, J.: On the statistical significance of climatic trends estimated from GPS tropospheric time series. Journal of Geophysical Research: Atmospheres, 123. https://doi.org/10.1029/2018JD028703, 2018). So, the main question is: how significant are the trend value differences between the different months? The discussion in lines 309-316 also seems to indicate that the found "seasonal" trend differences (and the shape presented) is not a consistent feature.

The uncertainties are indeed missing in Fig. 5 (Fig. 6 in new manuscript). We therefore added the maximum trend uncertainty to the figure. The error bar represents the month with largest uncertainty for each data set, even though some months have smaller uncertainties. Significant trends (usually with smaller uncertainties) are thus marked by filled dots. Please also note that the uncertainty of monthly means from TROWARA and GNSS has been adapted, because we assessed that the monthly uncertainty used is too small for a total uncertainty of GNSS or radiometer measurements. We therefore decided to add a systematic uncertainty based on results from Ning et al. (2016). The updated uncertainties result in slightly different trends, but the effect is small and the more realistic uncertainties justify the change. The manuscript has been changed as shown below, and the Figures have been adapted to the new trend values. We thank the referee for the constructive criticism, and we think that the reviewed uncertainty estimates and the changes in Fig. 5 (Fig. 6 in new manuscript) improved this section.

As monthly uncertainties σ_{mon}, we use for TROWARA and GNSS data

$$\sigma_{mon} = \sqrt{\sigma_{\bar{x}}^2 + \sigma_{sys}^2}, \tag{1}$$

where σ_{sys} is a systematic error and $\sigma_{\bar{x}}$ is the standard error of the monthly mean, given by

$$\sigma_{\bar{x}} = \sigma n^{-\frac{1}{2}}, \tag{2}$$

with the standard deviation of the monthly mean σ and the number of measurements per month n. The systematic error σ_{sys} is estimated to be 1 mm for TROWARA and $0.7\,\mathrm{mm}$ for GNSS data. These values are based on results from Ning et al. (2016a), who assessed IWV uncertainties from a radiometer and GNSS observations in Sweden.

Concerning the length of the time series, please note that the length of the time series is considered in the uncertainty of the trend estimate. A special characteristic of the trend tool we use is the consideration of the full data error covariance matrix instead of the mere error bars of the data. The trend uncertainty is estimated using generalized Gaussian error propagation in a sense that the dependence of the model parameters (trend, amplitudes of the components of the annual cycle) on the uncertainties of the ingoing data are calculated. The autocorrelated error components are estimated from the autocorrelation of the fit residuals. The necessary length of the time series depends on the included sources of variability. The more drivers of variability (e.g. overtones of annual cycle) are included in the trend model, the smaller the autocorrelated parts of the fit residual will be, and the better is the reliability of even a quite short time series. This is true as long as the number of data points is large enough to allow the fit of the related increasing number of model parameters, which is the case for our time series.
The significance of the trend differences between different months can be estimated as follows: The estimated error variances of the trends of both months under consideration are added to give the sum of the estimated variances. The square root of this is the estimated standard deviation of the difference. The trend difference can then be divided by this standard deviation. If this quotient is larger than 2, assuming Gaussian error statistics, the significance is approximately 5% (95% confidence limit). In our case, this test shows that only the difference between MERRA-2 trends in November and December is significantly different at 95% confidence interval. For the higher summer trends and the trend peak in October, we can be confident at 68% (1σ) that they differ from the trends of the other months (for TROWARA and reanalysis data). We therefore added a sentence to indicate this.

However, the differences between those monthly trends are significant only at 68% confidence level.

Beyond this, we would like to stress that we do not claim that our trend estimates have any validity outside the time period analysed. We do not endorse extrapolation. We restrict our analysis to descriptive statistics of the data available.

1.2 Specific comments

> *Page 1, lines 20-21: rephrase "it builds the link between temperature and precipitation" , building the link sounds awkward*

Modified.

[...] water vapour is involved in important tropospheric processes such as cloud formation~~, it builds the link between temperature~~ and precipitation [...]

> *Page 2, line 42: specify in which wavelength range the satellites that are restricted to oceans only operate.*

The text was adapted as follows.

Second, **visible and infrared satellite techniques are limited to clear-sky measurements. Further,** ~~many~~ satellite products from **passive mircowave sensors** are restricted to oceans only, because the well-known ocean surface emissivity makes retrievals generally easier over oceans than over land surfaces (Urban, 2013).

> *Page 2, line 47: drop "probably" in the sentence "Radiosondes probably provide the longest time series, ..."*

Modified.

> *Page 5, lines 147-148: it is a pity that you use the Bevis approximation to estimate Tm from Ts, while you could have used the ERA5 vertical profiles of temperature and specific humidity to calculate them. You might comment on the applicability of the Bevis approximation for Switzerland.*

We agree that alternatives to the Bevis approximation exist. However, we prefer not to use the ERA5 vertical profiles in order to keep the GNSS IWV data independent from ERA5. This is especially important because we compare the GNSS data with ERA5 data for validation.
Further, Alshawaf et al. (2017) showed that the use of reanalyses temperature and pressure data can lead to a bias in IWV compared to the use of surface measurements, especially in mountainous regions in Germany. We therefore follow their recommendation to use the Bevis approximation derived from surface temperature. We think that for the current study, the required additional effort by changing the retrieval would be larger than the benefit. Nevertheless, we will consider using a more advanced approach to determine the mean temperature at the GNSS stations in future.

Page 8, lines 237-238: explain what the impact of an antenna and receiver change might have on the data variability. I understand that these changes might cause a jump in the mean of a time series, but it is less clear to me how they might cause a higher/smaller data variability. Please comment on this.

We agree that a receiver or antenna change is not directly linked to the data variability. The antenna was enhanced from GPS only to GPS and GLONASS, which might improve the tropospheric values. It is nevertheless questionable if this can effect the data variability. We therefore adapted the statement as followed.

The anomalies are less variable from 2007 to 2012, but it is not clear whether this is related to the antenna update in 2007.

Page 8, lines 239-240 and Fig. 2b: which differences are you referring here to? GNSS – ERA5 or ERA5 – GNSS. Please specify.

As indicated in the caption of Fig. 2, we compute the relative difference with ERA5-GNSS/GNSS. We adapted the text for clarification.

Furthermore, the relative difference to ERA5 **((ERA5 - GNSS)**/**GNSS)** reveals a data jump [...]

Page 9, lines 264-and following: when comparing the IWV trends of TROWARA with the GNSS IWV trends, please mention if these trends are calculated for the same time periods, and if not, what the impact of the time period on the calculated trend is.

The GNSS trends are estimated for a shorter time period than TROWARA and the reanalyis trends. We now mention this in the manuscript, referring to Table 1. As discussed in the general comment, the trend length might have an effect on the trend estimate, but is considered in the trend uncertainties. Note also, that for TROWARA, starting in 2000 instead of 1995 has quasi no effect on the trend estimate.

Reanalysis IWV at Bern increases significantly by $3.7\,\%$ per decade for MERRA-2 and by $2.3\,\%$ per decade for ERA5 data**, both for the period from 1995 to 2018**. [...]
The larger GNSS trend uncertainties compared to TROWARA and reanalysis trends are mainly due to the bias correction, which adds some uncertainty to the trend estimates. Further, all GNSS trends result from a shorter time period than TROWARA and reanalysis trends (see Table 1), which also increases the trend uncertainty and may lead to some trend differences.

Page 10, lines 291-292: to which GNSS stations with deviating trend values, due to instrumental issues are you referring here to? I guess not to Payerne, since the radiosonde measurements give trend values close to the GNSS IWV trends, no? Please specify the GNSS stations here.

We were mainly refering to the EXWI trend, but we agree that the sentence is not clear in this summary and we removed it.

~~Some GNSS stations deviate from these trend values, probably due to instrumental issues.~~

Page 10, line 307-308: I don't understand this argument: strictly speaking, a (constant) bias between datasets will not have an impact on the trend difference between those datasets. Please explain.

As mentioned in the last paragraph of section 4, the larger difference between MERRA-2 and TROWARA data in winter mainly occurs in the last decade, after 2008. This suggests, that TROWARA observed more IWV in winter than MERRA-2 in the last decade, whereas this feature was less visible in the years before. It is therefore not a constant bias and can be reflected in different winter trends. We adapted the text as follows.

This larger disagreement between TROWARA and reanalysis trends in December and January is consistent with the larger winter biases of TROWARA **starting in 2008** in Fig. 3c (Fig. 4c in new manuscript).

Page 12, line 345: this argument can be easily checked: do the same analysis for the reanalysis grids neighboring the used reanalysis grids at Bern. Please do so.

As suggested, we investigated additionally monthly reanalysis trends for the used reanalysis grids. Indeed, they differ only slightly from the trends at the Bern grid, and are therefore not a main argument to explain differences between reanalysis and GNSS trends. We therefore removed these argument in the text and thank the referee for the remark.

p. 10, l. 304: ~~Most of the used GNSS stations are not located within the Bern reanalysis grid, which might explain some of the trend differences. The better agreement in summer suggests that the spatial difference is less critical in summer conditions.~~

p. 11, l. 345: ~~which might again partly be explained by the spatial difference of most GNSS stations to the used reanalysis grids at Bern.~~

Page 12, lines 346-following: as mentioned as a general comment: in this discussion, I was asking myself what the impact was on the constant RH approximation on the results of this analysis.

We modified Fig. 5 (Fig. 6 in new manuscript) showing monthly trends around Bern, and added also RH trends from ERA5 to the figure. The text and interpretation have been adapted accordingly.

This discrepancy can be related to changes in RH, which was assumed to be constant (Eq. (9)). Indeed, our trends of ERA5 RH for the Bern grid (Fig. 6c) show that RH was not constant in those months, especially in winter but also in May and June. Even though the RH trends are not significantly different from zero, these results suggest that assuming RH to be constant may not be valid during all seasons, especially in winter. This makes the attribution of IWV trends to changes in temperature more challenging.

Page 12, line 365: here, but also at other places in the manuscript: please use the word "bias" only if you mention your reference. It is not clear from this sentence here if GNSS is biased low w.r.t. FTIR or if FTIR is biased low w.r.t. GNSS.

Modified as followed.

~~A mean FTIR bias of~~ $\cancel{-0.26 \pm 0.3\,\mathrm{mm}}$ ~~is found when comparing monthly means of coincident GNSS and FTIR measurements. [...] Compared to the fully sampled GNSS time series, we found a bias of~~ $\cancel{1.05 \pm 0.61\,\mathrm{mm}}$

~~(GNSS – FTIR), which corresponds to a bias of 34 % (using the mean of the fully sampled GNSS as reference).~~

Monthly means of coincident GNSS data have a mean dry bias of $-0.26 \pm 0.3\,\mathrm{mm}$ compared to FTIR ($\mathrm{GNSS_{coincident}} - \mathrm{FTIR}$) (Fig. 7c). Further, monthly means of fully sampled GNSS have a bias of $1.05 \pm 0.61\,\mathrm{mm}$ compared to FTIR (GNSS – FTIR), which corresponds to a bias of 34 % (using the mean of the fully sampled GNSS as reference).

Page 12, lines 371-377: as the IWV amounts at Jungfraujoch are very low, there might be another argument for the GNSS dry bias w.r.t. FTIR: as pointed out by Wang et al. (2007), under dry conditions, the GPS is less sensitive to low IWV values as other devices (reference: Wang, J., Zhang, L., Dai, A., Van Hove, T., and Van Baelen, J.: A near-global, 2-hourly data set of atmospheric precipitable water from ground-based GPS measurements, J. Geophys. Res., 112, D11107, doi:10.1029/2006JD007529, 2007). Please comment.

We thank the referee for this indication. We checked the mentioned reference and also the COST report (Bock et al., 2020, p. 343) and added the comparison with Schneider et al. (2010) to the manuscript.

[...] the remaining bias of $-0.26 mm$ when using coincident GNSS measurements indicates that GNSS measures slightly less IWV than FTIR. **This is consistent with results from Schneider et al. (2010), who report that GNSS at the high altitude Izaña Observatory (Tenerife) systematically underestimates IWV in dry conditions (**$< 3.5\,\mathrm{mm}$**).** ~~This result is consistent with previous studies that reported negative GNSS biases compared to~~ **Further, a dry bias has also been observed in previous studies that compared Jungfraujoch GNSS data with** Precision Filter Radiometer (PFR) data (Guerova et al., 2003; Haefele et al., 2004; Morland et al., 2006; Nyeki et al., 2005).

Page 13: the word "astonishingly" is not very scientific

Modified.

From this point of view the achieved results are ~~astonishingly~~ good **and** a possible offset is not relevant for trend analyses as long as it is constant over the whole trend period.

Page 13, line 387: what is the trend estimate of the GNSS time series that coincides with the FTIR time series?

The trend of GNSS data that coincides with FTIR measurements is 0.05mm per decade, which is similar to the FTIR trend (0.04mm per decade). We do not show this information in Fig. 7 to avoid overload, but we adapted the text accordingly.

The difference between both trends ~~might~~ **can** partly be explained by the dry sampling bias of the FTIR spectrometer, that measures only during clear-sky day conditions. **Indeed, the absolute GNSS trend is comparable with the FTIR trend when we use GNSS data coincident with FTIR measurements, with** $0.05\,\mathrm{mm}$ **per decade (not shown).**

Page 13, line 407: there's a typo in "autumn"

Modified.

Page 14, lines 411-412: as already mentioned in the general comments: how many years do you need to obtain "stable" trends?

As discussed in the general comment, it depends on the included sources of variability in the trend programme. We have shown that the trend uncertainty does not only depend on the length of the time series, but also on the number of change points in the time series. Our trend error estimates include the precision of the data, bias uncertainty between measurement periods after antenna updates, and atmospheric processes not accounted for by the trend model and thus showing up as auto-correlated fit residuals. They do not include nonlinear atmospheric variability on timescales longer than our analysis period. The latter are aliased into our linear trend. Thus our results should be understood as descriptive statistics only and should not be used to extrapolate beyond our analysis period.

Page 15, lines 454-455: the large spatial variability between the different grids in es changes in Merra-2 is surprising, especially when comparing with ERA5, which have a higher spatial resolution. What is the explanation for this?

We assume that the large spatial variability in MERRA-2 e_s changes is due to the poor representation of the topography in the Alpine region, and thus lacking local dynamics, which results in underestimated temperature (compared to ERA5). Further, we found that this underestimation is reduced starting at around 2017, which leads to a jump in the MERRA-2 time series resulting in a very strong trend. We assume that this is related to a MERRA-2 model improvement in recent years (e.g. improved topography, changes in assimilated data) and adapted the manuscript accordingly.

In contrast to ERA5, The MERRA-2 changes in e_s show large spatial variability, with strong differences between different grids and generally larger values in the Alpine region. **These large values are caused by a jump in MERRA-2 tropospheric temperature data around the year 2017 in the Alpine grids, which results in strong temperature trends. This might be due to MERRA-2 model changes in topography or assimilated data. In the Alpine region** ~~On regional scales~~, the MERRA-2 changes in e_s (Fig. 14) thus differ strongly from the MERRA-2 IWV trends (Fig. 12).

To summarize, the reanalysis IWV trends follow on average the changes expected from temperature changes~~, but~~. **However** MERRA-2 shows large regional variability for changes in e_s ~~based on lower tropospheric temperature changes.~~ **due to biases in lower tropospheric temperature data in the Alpine region**.

Conclusions: The reanalysis grids probably miss regional variability in atmospheric stratification and convection, as it was also observed for zonal means by Wentz et al. (2000). **Further, a bias in MERRA-2 tropospheric temperature was observed for several Alpine grids after 2017.**

Page 16, lines 460-461: this statement can be easily verified: what is the winter temperature trend in the 1995-2018 interval?

A simple linear trend analysis of MeteoSwiss surface temperature data (doi: `10.18751/Climate/Timeseries/CHTM/1.1`) confirms this statement. Whereas the temperature trend is positive for long-term winter temperature observations (e.g. starting in 1961), it is negative for the shorter study period from 1995 to 2018. We therefore adapted the text as follows.

This difference is ~~probably~~ due to our short study period. A few cold winters in the past 15 years ~~might~~ have hidden the overall positive temperature trend when looking only at the relatively short period from 1995 to 2018 (MeteoSwiss, 2019).

> *Page 28, Fig. 4: The datasets that have the smallest trend uncertainties (the reanalyses) are actually the ones of the course time evolution (monthly means), while GNSS data were available as hourly values, if I remember it correctly. Please comment on the trend uncertainties obtained here in this perspective.*

The GNSS data have indeed hourly resolution, but we use monthly means for the trend estimation. The initial resolution should therefore have little to no effect on the trend estimate. We think that the larger GNSS uncertainties are mainly due to the bias correction, which adds some uncertainty to the trend estimate, and due to the shorter time series. We added this explanation to the manuscript.

The larger GNSS trend uncertainties compared to TROWARA and reanalysis trends are mainly due to the bias correction, which adds some uncertainty to the trend estimates. Further, all GNSS trends result from a shorter time period (see Table 1) than TROWARA and reanalysis trends, which also increases the trend uncertainty and may lead to some trend differences.

2 Author's response to referee #2

2.1 General comment

> *This manuscript investigates the consistency of monthly means and linear trends of IWV from ground-based radiometry, FTIR, and GNSS data, and two modern reanalyses (ERA5 and MERRA-2) in Switzerland for the period 1995 to 2018. This study is of special interest to the climate community because it confronts several state of the art observational techniques and two of the currently best available reanalyses which assimilate a huge amount of observations (mainly from satellite remote sensors). Though the investigation is limited to the country of Switzerland, it shall shed some light on the uncertainties that generally impact both types of climate data and propose a methodology that may be replicated to other regions of the world. One specific source of uncertainty in trend analysis resides in the treatment of inhomogeneities in the data due to changes in the observing systems. In this respect the approach described by the authors with the GNSS data is original in the sense that it adjusts offsets (so-called jumps) in the time series that may be due to antenna and station changes. Though the proposed approach is interesting I think the way this issue is handled it is also the main weak point in the study.*

Thank you for this positive feedback and the constructive criticism, to which we respond in the following comments.

> *The approach of fitting simultaneously biases (or changes in the mean) and a linear trend is an ill- posed problem which requires special care and validation because of collinearity. Indeed, it is well known that these parameters are highly correlated, e.g. successive downward changes in the mean can be compensated by an upward trend hence over-estimating (underestimating) an existing positive (negative) trend in the series. Interpreting the trend parameter alone may thus lead to erroneous conclusions. Though the authors notice in several places that the trends after bias correction increase, they do not consider it as problematic, e.g. at NEUC the GNSS trend increases from 0.33 to 0.74 mm/decade when 3 jumps are adjusted and at PAYE the trend increases from 0.32 to 1.14 mm/decade after bias correction (when 3 jumps are fitted). It is noticeable that the uncorrected trends are in very good agreement with the ERA5 trend at Bern (0.34 mm/decade). Inspecting the station information table cited by the authors, reveals that 6 out of the 7 stations listed in Table 2 are subject to 3 or more jumps. The trends at all these stations are relatively high (above 0.58 mm/decade). One exception is station EXWI which did not undergo a bias correction and which has the smallest trend (0.02 mm/decade). It may be pure coincidence, but this point needs to be checked.*

It is true that most bias corrected trends are larger than the uncorrected trends. On the one hand, this can be due to positive biases in earlier years (or negative biases in later years), which leads to smaller trends if the bias is not corrected.
On the other hand, from the perspective of the trend model, this behavior tells us that the trends in each individual data block (after antenna updates) are larger than the overall (uncorrected) trend. The overall uncorrected trend is then assumed to be too small, due to unconsidered biases between the data blocks. If a large bias is allowed (large bias uncertainty), the total trend tends to be the average of the individual trends of each data block. The algorithm then corrects the difference between the mean values of the blocks because they are biased to each other. Conversely, if a small bias correction is allowed (smaller bias uncertainty), the block differences contribute more to the trend estimate, and the intra-block trends have less weight. We chose a realistic bias uncertainty of 5% (see Sect. 3.1.1), which restricts the bias

correction to a realistic magnitude. The corrected trend is thus accounting for the biases between the data blocks, without giving the individual block trends too much weight. Therefore, the fact that the corrected trends are mostly larger than the uncorrected trends just means that the trends within the blocks are larger than the overall (uncorrected) trend. The latter, however, can be falsified (too small) because of the biases. The trend uncertainty of this corrected trend will be larger, which reflects the fact that the intra-block trends are less reliable than the overall trend would be.

> *[...] The large dispersion in the GNSS trend estimates over Switzerland (Fig. 8) compared to the relative flatness of the reanalysis trends (Fig. 10) is striking as well and may further support this problem.*

The newly added uncorrected trends in Table 2 show that the dispersion of uncorrected trends is not smaller than for the corrected trends. However, the trend values are often slightly larger, as discussed above.

> *I suggest that the authors further investigate the impact of the bias correction procedure on the GNSS trends and possibly reduce it.*

To better asses the bias correction, we added a section to the manuscript (Sect. 3.1) where the approach is illustrated with an artificial time series. We think, this better illustrates the effectiveness of the approach in correcting possible biases in a data set and justifies the use of the approach for the GNSS data.

The approach is illustrated with an exemplary case (Fig. 2). We used an artificial time series with a trend of $0.5\,\mathrm{mm}$ per decade, and added three change points with a constant bias for each subset. The change points represent for example an instrumental update, that leads to a constant bias in the following data. The biased time series has a trend of $1.19 \pm 0.06\,\mathrm{mm}$ per decade, which is too large compared to the true trend of $0.5 \pm 0.06\,\mathrm{mm}$ per decade. To improve the trend estimate, we add a fully correlated block in S_y for each biased subset, assuming a bias uncertainty of 5 %. We obtain a corrected trend of $0.52 \pm 0.17\,\mathrm{mm}$, which corresponds within its uncertainties to the true trend of the unbiased time series. This demonstrates that the approach can reconstruct the true trend from a biased time series, with slightly increased trend uncertainties.

Further, we assessed the monthly uncertainties that were used for GNSS trends as being too small (only 1.5%), and added a systematic uncertainty of 0.7 mm to all GNSS monthly uncertainties, leading to monthly uncertainties of around 5% (see comment P7L200 below). This gives the algorithm some more liberty in the bias fit, which leads to a slightly smaller bias correction at some stations (e.g. trend of 7% in Payerne instead of 7.3% before). We think, this change is justified and the bias correction is improved.

> *One critical aspect here is with the position of the change points. A misplaced change point, or a change point inserted in a series where there is no jump, is very likely to bias the trend estimate. So it is of prime importance to detect and correct only the true change points. It is not clear from the manuscript how the jumps are detected. Is it from the station position time series? The authors should be careful that though some jumps in the position time series may have a coincident jump in the ZTD or IWV time series, this is not always the case. The reason is that, e.g. in the case of an antenna change, a station height offset can be due to both a PCO and a PCV change while a ZTD offset is mainly due to a PCV change (as long as*

the position is estimated simultaneously with ZTD). Only when change points are properly detected can the method of estimating biases and trends together provide accurate trend estimates.

A changepoint was introduced as soon as an antenna has been replaced, even if it would not be visible in the coordinate time series. In the trend programme, the bias due to a changepoint in the data is fitted from the data itself. If we assume a jump even though the data do not show an offset (for example due to a PCO change that does not lead to a change in ZTD), the bias fit from the data would detect no jump and therefore not correct for it. A misplaced changepoint does thus not impact the trend itself. Only the uncertainty of the trend would be increased. This has been verified with an artificial time series, where we added a changepoint even though no jump in the data was observed. The trend estimate did not change, only the uncertainty increased slightly in the corrected trend. Thus, the bias correction method is a practical and objective tool for trend analysis of GNSS IWV series with possible jumps.

In order to provide proper insight into the impact of the correction, it would be useful to show the trends estimated from corrected and uncorrected time series.

We agree that showing the uncorrected trends gives a better insight into the impact of the correction. Therefore, we added the uncorrected trends for the GNSS stations around Bern in Table 2 and added the statement shown below. However, the uncorrected trends may be falsified due to the missing consideration of jumps after antenna updates. We therefore prefer showing only the corrected trends in the figures.

For comparison, the GNSS trends without bias correction are also shown in Table 2. They are generally smaller than the bias corrected trends, suggesting that GNSS trends are mostly underestimated when biases are not accounted for. Further, their uncertainties are smaller, reflecting the additional uncertainty when biases are considered.

For your information, we provide the GNSS trend map with uncorrected trends here in the author's response (Fig. AR.1). We observe that most uncorrected GNSS trends are smaller, and have smaller uncertainties than the corrected trends. This is consistent with the statement that we added to the manuscript and the uncorrected trends added to Table 2. Uncorrected trends are significant at several stations. We think, however, that this is not reliable, because possible biases due to the instrumental updates are not considered, trends might thus be falsified and uncertainties underestimated. This is confirmed by our example with the artificial time series (Fig. 2), for which a false trend value with a small uncertainty is derived when the bias correction is not applied. We therefore show only the corrected trends in the figures of the manuscript. We think that the newly added uncorrected trends in Table 2 as well as the example cases (Figures 2 and 3 in the new manuscript) are sufficient to give an idea of the impact of the correction.

I recommend thus that the GNSS offset correction be improved or at least carefully assessed and the manuscript revised accordingly. The conclusions may change significantly.

We think that our additional analysis with an artificial data set made a careful assessment of the bias correction approach possible. We think that our changes and this additional section improved the manuscript and thank the referee for this input.

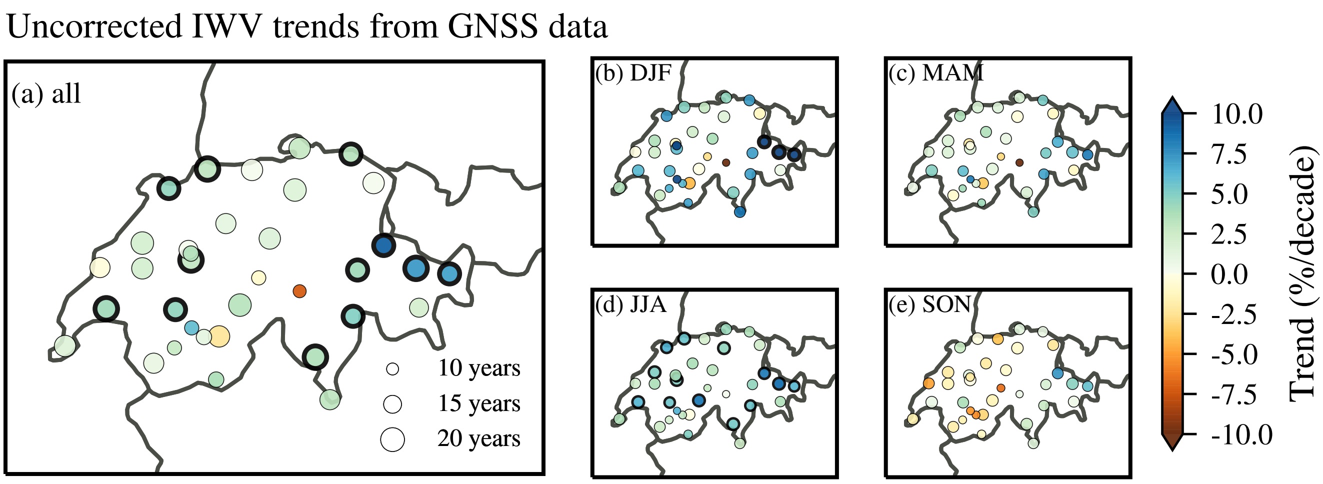

Figure AR.1: Uncorrected trends of IWV in Switzerland for the different GNSS stations for **(a)** the whole year and for the four seasons (**(b)** to **(e)**). The length of the GNSS time series is indicated by the size of the markers. Stations with trends that are significantly different from zero at 95% confidence interval are marked with a bold edge. Possible jumps in the time series due to GNSS antenna updates have not been considered in these trend estimates. The trends and their significance are therefore assumed to be not reliable. For the bias corrected trends, see Fig. 9 in the manuscript.

2.2 Minor comments

A number of additional specific comments are given below regarding other aspects of the work and the manuscript.

P4L99: could there be an effect of the changes of the TROWARA instrumentation in 2002 and 2004 on the IWV data and IWV trend estimated with the radiometer? Is there a bias adjustment similar to that applied to the GNSS data or any kind of recalibration?

Change points in TROWARA data due to instrumental changes before 2009 have been detected and corrected by a careful comparison of the TROWARA time series with a co-located weather station (Morland et al., 2009). No instrumental changes have been performed in recent years. We therefore presume that the data is well homogenized and use no bias correction in the TROWARA trend estimates.

Section 2.3: why did the author use the outdated Thayer constants and Bevis formula for the ZTD to IWV conversion? More elaborate and updated approaches are given in the COST GNSS4SWEC final report (see e.g. Chapter 6, Section 6.4.2). Note that the older refractivity constants may be responsible for a small bias in the GNSS IWV when comparing these data to other well calibrated observations (e.g. microwave radiometer and FTIR) and that ZHD and Bevis Tm computed from surface Ts observations and Ps may produce spurious diurnal and seasonal signals in the GNSS IWV estimates (due to spatial extrapolation errors and inaccuracies in the Bevis formula).

We thank the referee for the suggestions of updated approaches for the ZTD to IWV conversation. We will consider using these newer approaches in future studies. We agree that the use of old refractivity constants may result in a bias in IWV, as shown in the mentioned GNSS4SWEC report (Bock et al., 2020). However, a possible bias which is constant in time would not affect the trend estimates. We therefore think that the approach used in our study is sufficient for the main purpose of our study, which is trend estimation.

Concerning surface pressure as well as surface and mean temperature data, we prefer to stay independent from reanalysis data, because we compare the GNSS data with reanalyses for validation. Also, the use of reanalysis data for the determination of T_m, T_s and p_s can lead to a bias, especially in mountainous areas, as shown by Alshawaf et al. (2017). We are aware of possible inaccuracies in the current approach and will consider using more advanced approaches in future studies. However, we think that for the current study, the required additional effort when reprocessing the whole data would be larger than the benefit.

> *P7L200: what does this standard deviation represent exactly? Is it the variability of the IWV data at the nominal time sampling (in this case what is the sampling of the GNSS IWV data? 1 hour?) or is it a formal error?*

The standard deviation used represents the variability around the monthly mean. We adapted the text to clarify this. The standard error depends indeed on the sampling. The time sampling of TROWARA is of several seconds (see Sect. 2.1), the GNSS sampling is 1 hour (see Sect. 2.3). For both datasets (TROWARA and GNSS), the standard error used for each monthly mean is around 1.5%. Within the review process, we assessed that this monthly uncertainty is too small for a total uncertainty of GNSS or radiometer measurements. We therefore decided to add a systematic uncertainty based on results from Ning et al. (2016). These new uncertainties are around 8% for TROWARA and 5% for a typical GNSS station. The updated uncertainties result in slightly different trends, but the effect is small and the more realistic uncertainties justify the change. The manuscript has been changed as shown below, and the Figures have been adapted to the new trend values.
For consistency, we also added the approximated value of FTIR uncertainties used. The FTIR uncertainties are much larger due to the low number of measurements per month and the model fit to obtain monthly means from the sparse data, as described in Sect. 2.2. We also add a sentence on the uncertainty used for the newly computed RH trends (10%) and for temperature trends (around 2.5K).

As monthly uncertainties σ_{mon}, we use for TROWARA and GNSS data

$$\sigma_{mon} = \sqrt{\sigma_{\bar{x}}^2 + \sigma_{sys}^2}, \tag{3}$$

where σ_{sys} is a systematic error and $\sigma_{\bar{x}}$ is the standard error of the monthly mean, given by

$$\sigma_{\bar{x}} = \sigma n^{-\frac{1}{2}}, \tag{4}$$

with the standard deviation of the monthly mean σ and the number of measurements per month n. The systematic error σ_{sys} is estimated to be 1 mm for TROWARA and $0.7\,\mathrm{mm}$ for GNSS data. These values are based on results from Ning et al. (2016a), who assessed IWV uncertainties from a radiometer and GNSS observations in Sweden. Our monthly uncertainties used for TROWARA and GNSS are on average 8 % for TROWARA and around 5 % for a typical GNSS station. FTIR uncertainties (around 25 %) are based on the model fit of daily means as described in Sect. 2.2. [...]
In addition to IWV trends, we determine reanalysis trends of RH (ERA5) and temperature (ERA5 and MERRA-2). We use monthly uncertainties of 10% to estimate RH trends, whereas the standard error of each averaged temperature profile (below 500 hPa) is used as monthly temperature uncertainties (around 2.5 K).

Why is the standard deviation of TROWARA 2 or 3 times smaller than the GNSS standard deviation? (is it because of the time sampling?)

The larger trend uncertainty for the GNSS stations is not due to the assumed data uncertainty (which is similar to TROWARA, see comment before), but rather due to the shorter time series and the bias fitting which adds some uncertainty.

P8L221: explain how the jumps are detected (see also the general comments).

A changepoint was introduced whenever a site antenna was replaced. A changepoint is also introduced when a jump would not be visible in the corresponding coordinate time series (especially station height). We adapted the manuscript to make this clearer. In rare cases, jumps were also set up when coordinate jumps were visible in the coordinate domain without an antenna change. Reasons for this are sometimes difficult to find out, but e.g. tree cuts or new buildings very close to the station may result in a different observation skyplot.

We introduced change points in the trend programme as soon as ~~antenna updates have led to~~ a **possible** jump in the GNSS data **has been** ~~as~~ recorded by swisstopo (available at `http://pnac.swisstopo.admin.ch/restxt/pnac_sta.txt`), **which is mostly due to antenna updates**.

Fig. 2b: how does the corrected GNSS time series compare to the ERA5 data? Are the biases reduced?

In the corrected GNSS time series, the jump in the ERA5-difference is reduced. We added this corrected difference to ERA5 in Fig. 2b (Fig. 3b in new manuscript).

When the bias is considered in the trend model, **the jump in the difference to ERA5 is reduced (Fig. 3b). Further,** we obtain a larger bias corrected trend [...]

P9L269: compared to the TROWARA trends which are of similar magnitude, the GNSS trends are not deemed significant because the standard deviation is 2 or 3 times larger. This prompts again for a clarification on the reason of the difference in standard deviation.

The larger uncertainties in GNSS trends are mainly due to the changepoints in the time series due to antenna updates, which adds some uncertainty to the trend estimates. Further, GNSS time series are shorter, which also slightly increases the uncertainty of the trend estimate. Both points explain the larger GNSS trend uncertainties. We added this explanation to the manuscript

The larger GNSS trend uncertainties compared to TROWARA and reanalysis trends are mainly due to the bias correction, which adds some uncertainty to the trend estimates. Further, all GNSS trends result from a shorter time period than TROWARA and reanalysis trends (see Table 1), which also increases the trend uncertainty and may lead to some trend differences.

P9L271: this sentence is very speculative. Revise or remove.

We agree that this formulation is too vague and removed it.

~~However, the uncertainties of the monthly reanalysis data might be larger than the here used value of 10%, which would also lead to larger uncertainties of the reanalysis trends.~~

P9L274-275: The shorter time period of EXWI is suggested but WAB1 has a much shorter period. Revise or remove.

We agree and removed this sentence.

The quasi zero trend at the EXWI station is less reliable than the other trends, because the EXWI station ~~provides data in a shorter time period (until 2016). Further, it~~ is not part of the AGNES network and therefore does not fulfil the same quality requirements.

P9L279-284: is the reliability of radiosonde data good enough to estimate trends? Similarly, the lidar trends are probably biased because they include clear sky measurements only. Moreover, the time period for the latter is much shorter. I think these results can hardly be inter-compared. Please remove.

The reliability of radiosonde data for long-term trend analyses has been improved substantially with the homogenzitation efforts within the GCOS Reference Upper Air Network (GRUAN) (e.g. Dirksen et al., 2014). At Payerne, not all radiosonde profiles are GRUAN-certified, but Hicks-Jalali et al. (2020) showed that the difference between the homogenized GRUAN profiles and the operational radiosonde profiles lie within the GRUAN uncertainties, which justifies the use of the operational radiosonde data.
We agree that the short trend time period and a possible clear-sky bias of the lidar is a limitation of the study by Hicks-Jalali et al. (2020). However, the use of lidar data for water vapour retrieval is a new and promising technique, and we think that the comparison with the co-located GNSS data at Payerne is important. We therefore suggest to keep this short comparison, but added their limitations in the text as followed.

However, comparing their trend results with ours has to be done with care, because their trend time period is short and the lidar trends might contain a clear-sky bias.

P10L285-294: trend estimates computed for different periods must be compared with much care.

We agree that comparing trends of different periods has to be done with care. However, we think it is important to set our results in the context of previous studies that used the same TROWARA data set. We added a sentence to point out to the reader that care has to be taken.

However, care has to be taken when comparing these TROWARA trends of different trend period lengths.

P10L295: why would trends be larger in summer? Do you have any clue for this?

Absolute trends are largest in summer because more water vapour is available in summer. Relative trends might be larger in summer due to increased evaporation with increasing temperature. Hocke et al. (2019) showed that evaporation of surface water in Bern plays a major role in summer. Surface evaporation is temperature dependent, which might explain larger IWV summer trends due to a warming climate. IWV trends largest in summer have also been observed in China (Peng et al., 2017) or in Sweden (Nilsson et al., 2008). Further, we have shown that summer trends are consistent with the temperature increase in summer, as discussed in Sect. 4.2.

Fig. 5: what is the benefit of using the mean GNSS trend here? how is this mean computed?

The arithmetic mean of trends from GNSS stations close to Bern is shown in Fig. 5 (Fig. 6 in new manuscript). We decided not to show all individual GNSS trends to avoid an overload of the figure. The monthly trends of the different GNSS stations close to Bern show a similar "shape" throughout the year. Therefore, the arithmetic mean is a good representation of those GNSS trends. The Figure caption has been adapted to clarify the mean computation.

Figure 5. Trends of IWV for different months for TROWARA in Bern, GNSS stations close to Bern **(arithmetic mean)**, and reanalysis grids (MERRA-2 and ERA5) at Bern.[...]
The mean trend (arithmetic mean) of the GNSS stations around Bern agrees with the other data sets in summer, [...]

Fig. 5: Add error bars on the monthly trend estimates to judge whether the variations are significant or not.

Error bars have been added to Fig. 5 (Fig. 6 in new manuscript). The error bars represent the month with largest uncertainty for each data set. Some months have smaller uncertainties. Significant trends (usually with smaller uncertainties) are thus marked by filled dots. A sentence about the significance of the monthly trend differences has been added (see also general comment of referee 1).

However, the differences between those monthly trends are significant only at 68% confidence level.

Fig. 5: The GNSS trend for March is suspicious and needs to be checked.

This strong negative averaged March trend is mainly due to strong negative trends at the EXWI station. However, also all the other stations around Bern show smaller March trends than reanalysis data. The reason for this negative GNSS March trend is not clear.

P10L304: The fact that the GNSS stations are not located in the same reanalysis grid (ERA5 or MERRA-2?) does not sound like a good explanation for the differences. Please revise or remove.

We investigated monthly reanalysis trends for the used reanalysis grids. Indeed, they differ only slightly from the trends at the Bern grid point, and are therefore not a main argument to explain differences between reanalysis and GNSS trends. As suggested, we removed this argument in the text and thank the referee for the remark.

p. 10, l. 304: ~~Most of the used GNSS stations are not located within the Bern reanalysis grid, which might explain some of the trend differences. The better agreement in summer suggests that the spatial difference is less critical in summer conditions.~~
p. 11, l. 345: ~~which might again partly be explained by the spatial difference of most GNSS stations to the used reanalysis grids at Bern.~~

P11L315: mention that the temperature trends explain part of it and that they are further discussed in section 4.2.

We thank for this adequate remark and adapted the manuscript as followed.

Nevertheless, we showed that the IWV trend peak is consistent with November temperature trends, suggesting that those trends are temperature driven (see Sect. 4.2 and Fig. 6).

> *P11L325-328: contains some inaccuracies. Suggested correction: "In case that the water vapour pressure e is smaller than es, the available water is in vapour phase, whereas for e > or = es it condenses. With increasing temperature, es increases, which leads for a given relative humidity (RH) to an increase of water vapour e. Changes in es can therefore directly be compared to changes in the amount of water vapour measured by e or IWV, assuming that the RH remains constant"*

Thank you for this clarification, we adapted the text as followed.

In case that the water vapour pressure e is smaller than e_s, the available water ~~evaporates~~ **is in vapour phase**, whereas for $e \geq e_s$ it condenses ~~until it reaches the equilibrium ($e = e_s$)~~. With increasing temperature, e_s increases, which leads for a given **relative humidity (RH)** to an increase of e ~~water vapour in the vapour phase~~. Changes in e_s can therefore directly be compared to changes in the amount of water vapour **assuming that RH remains constant [...]**

> *P11L325-328: Give a reference to other studies concluding that RH remains nearly constant and be more specific about the conditions for this to hold, namely is this result valid at regional scale?*

The assumption of fixed RH has been presented by Möller (1963), and Held et al. (2000) discusses the usefulness of this assumption to evaluate water vapour feedbacks. We added these references to the manuscript. Note that following the suggestion of referee 1, we added a full analysis of ERA5 RH trends, indicating that RH seems not to be constant in all seasons. The validity of the assumption is thus further discussed in Sect. 6.2 and 7.

[...] assuming that RH remains constant **(Möller, 1963; Held and Soden, 2000)**

> *P12L347-355: I am not convinced of the impact of temperature inversions. Do you have further evidence of this? Instead, the effect of moisture transport is a better explanation (e.g. also discussed by Parracho et al., 2018).*

We agree that this assumption would require further evidence, e.g. additional analyses. We have shown that inconstant relative humidity can partly explain the observed discrepancies in winter monhts. Further, we agree that moisture transport may be a more dominant factor. We think that those 2 aspects are sufficient to explain the observed differences and therefore removed the assumption of winter temperature inversions.

~~This discrepancy might be related to temperature inversions that are often present in winter. In these situations, the surface water vapour is trapped by the inversion and less propagating in the free troposphere (Fujita and Sato, 2017), which means that the water vapour content does not scale anymore to temperature above the inversion layer.~~

P13L392: could the snow and icing problems effect the GNSS data used in this study?

As mentioned in Sect. 5, the old antenna (before 2016) at Jungfraujoch was never calibrated, because the special heated radome construction to avoid icing made the calibration complicated. The authors in the mentioned study (Nyeki et al., 2019) also refer to this problem, which is related with the snow and icing at Jungfraujoch. We reformulated the sentence to make their intention clearer. We account for this antenna change in the trend estimate by the bias correction.

They decided not to use GNSS IWV data from Jungfraujoch due to the high IWV variability and **the missing calibration of the antenna before the replacement in 2016.**

P13L403: is it 3 or 4 stations?

Corrected, it is three stations.

Only ~~four~~ **three** stations (~~11~~9 % of all stations) show negative IWV trends [...]

P14L410: trends computed for different periods and regions must be compared with much care.

We agree that comparing GNSS IWV trends from different regions and periods can be problematic. However, we think that it is important to put our results in the context of other GNSS based trend results in Europe. We therefore keep this comparison, but add a sentence about the problematic of comparing trends of different lengths.

Note, however, that both studies use different trend periods lengths than in our study, which makes trend comparisons difficult.

Fig. 13: these plots are weird. It seems that there is glitch in the data computation here. Please check carefully. Otherwise, a proper explanation of the MERRA-2 results should be given.

We investigated the MERRA-2 lower tropospheric temperature data in more detail. From Fig. 13 (Fig. 14 in new manuscript), it is evident that the unrealistic high MERRA-2 temperature trends occur mainly in grids with complicated topography (Alps). In those grids, the topography is poorly represented, which leads to lacking local dynamics and to biases in tropospheric temperature. We have seen that in all grids where the MERRA-2 temperature trend is large, the temperature is substantially underestimated compared to ERA5. However, this underestimation is reduced for all grids starting at around 2017, which leads to a jump in the MERRA-2 time series resulting in a very strong trend. We assume that this is related to a MERRA-2 model improvement in recent years (e.g. improved topography, changes in assimilated data). We adapted the manuscript accordingly.

In contrast to ERA5, The MERRA-2 changes in e_s show large spatial variability, with strong differences between different grids and generally larger values in the Alpine region. **These large values are caused by a jump in MERRA-2 tropospheric temperature data around the year 2017 in the Alpine grids, which results in strong temperature trends. This might be due to MERRA-2 model changes in topography or assimilated data. In the Alpine region** ~~On regional scales~~, the MERRA-2 changes in e_s (Fig. 14) thus differ strongly from the MERRA-2 IWV trends (Fig. 12).
To summarize, the reanalysis IWV trends follow on average the changes expected from temperature

changes~~, but~~. **However** MERRA-2 shows large regional variability for changes in e_s ~~based on lower tropospheric temperature changes.~~ **due to biases in lower tropospheric temperature data in the Alpine region**

Conclusions: The reanalysis grids probably miss regional variability in atmospheric stratification and convection, as it was also observed for zonal means by Wentz et al. (2000). **Further, a bias in MERRA-2 tropospheric temperature was observed for several Alpine grids after 2017. This reflects the problematic of using reanalysis data for trend estimates due to changes in observing systems or assimilated data.**

> *P15L444-445: I think it is not clear if it is the reanalyses results that are too smooth or the GNSS results that are too noisy. Can you clarify/discuss this point?*

The coarse resolution of the reanalysis grids is not capable to represent the topography correctly, especially in mountainous regions. As shown for example by Bock et al. (2005) or Alshawaf et al. (2017), reanalysis data can deviate substantially from GNSS data, especially in mountainous regions. If this bias is constant, it should not affect the trend estimates. However, spatial small-scale variability that is captured by GNSS stations and not by reanalyses might still lead to some differences in the trends. Further, it is evident that ungridded point measurements are more variable than gridded reanalysis data. To clarify this point, we adapted the text as followed.

However, the reanalyses do not resolve small scale variability, which can explain the differences to some GNSS station trends. **Further, the GNSS point measurements are generally more variable than the gridded reanalyses data.** Alshawaf et al. (2017) also observed larger differences in mountainous regions between GNSS derived IWV ~~trends~~ and reanalyses **data** in Germany.

> *P15L462-468: The uncertainty of the reanalyses is not directly addressed along in this work. So, drawing doubt on these data in the final discussion sound rather awkward. This being said, it is true that the use of reanalyses for trend analysis has been debated but the quoted references suggesting that ERA5 and MERRA-2 are more accurate at estimating trends are too general to support such an assertion. Please revise or remove this paragraph.*

We agree that the discussion of the reanalysis limitations and uncertainties is misplaced. We therefore moved it to the description of the reanalysis data sets in section 2.4. Further, we changed the formulation to respond to your suggestion.

When using reanalysis data for trend estimates, one has to keep in mind their limitations. Due to changes in observing systems of the assimilated data, the use of reanalyses for trend studies has been debated (e.g. Bengtsson et al., 2004; Dee et al., 2011; Parracho et al., 2018; Sherwood et al., 2010). ~~This problem has been addressed in the recent reanalysis products. Compared to the previous ECMWF reanalysis (ERA-Interim), the bias correction of assimilated data in ERA5 has been extended to more observation systems (Hersbach et al., 2018). Also MERRA-2 has been improved compared to the previous MERRA data, for example with reduced biases in the water cycle (Gelaro et al., 2017). Further analyses would be required to conclude if biases due to changes in observing systems still exist in the reanalysis data over Switzerland.~~ **The recent reanalysis products contain some improvements in handling possible steps in assimilated data. For example, the bias correction of assimilated data in ERA5 has been extended to more observation systems (Hersbach et al., 2018) and MERRA-2 reduced certain**

biases in water cycle data (Gelaro et al., 2017). Nevertheless, future studies have to assess whether these improvements affect the reliability of reanalysis data for trend estimates.

> *Fig. 10 and 11: to ease the comparison with GNSS results, add the GNSS results onto the reanalysis results. The plots may be resized.*

As proposed we added GNSS trends on the reanalysis IWV trend maps (Figs. 11 and 12 in new manuscript). We restricted the GNSS trends to stations with longest time series (18 or 19 years) to avoid the direct comparions with much shorter time series.

> *Table 1: add the number of jumps that are inserted in the trend analysis.*

The dates of change points have been added to Table 1.

3 Additional changes

In addition to the changes performed in response to the comments of the referees, we performed some small text changes, which are marked in the difference file, small figure layout changes as well as the following changes.

3.1 Modification of reference block in bias corrected trend estimation

During the tests with the artificial time series as described above, we found that the trend estimates can be further improved by a small modification in the trend estimation approach. We therefore decided to apply this change to our GNSS trend estimates and recalculated all our GNSS trends. The improvement consists of using the longest data subset as reference block (null-bias), which leads to slightly better estimates of the true trend. The reference block is the subset of the data for which no bias is assumed (null-bias). The biases for the other subsets of the data are estimated with respect to this block. Initially, we used the first subset (before the first change point) as reference block. However, this can lead to less good trend estimates, especially if the first subset is short (e.g. only a few months). We therefore recalculated all our GNSS trends, using always the longest subset as reference block in the covariance matrix. The new trend estimates are slightly different but they lie within the initial uncertainties.

3.2 Monthly uncertainties for temperature and RH data

The monthly uncertainties used to estimate temperature and RH trends have not been described so far and have been added to the methodology part.

In addition to IWV trends, we determine reanalysis trends of RH (ERA5) and temperature (ERA5 and MERRA-2). We use monthly uncertainties of 10% to estimate RH trends, whereas the standard error of each averaged temperature profile (below 500 hPa) is used as monthly temperature uncertainties (around 2.5 K).

4 References

Alshawaf, Fadwa, Kyriakos Balidakis, Galina Dick, Stefan Heise and Jens Wickert (2017). "Estimating trends in atmospheric water vapor and temperature time series over Germany". In: *Atmos. Meas. Tech.* 10.9, pp. 3117–3132. DOI: 10.5194/amt-10-3117-2017.

Bock, O., R. Pacione, F. Ahmed, A. Araszkiewicz, Z. Bałdysz, K. Balidakis, C. Barroso, S. Bastin, S. Beirle, J. Berckmans, J. Böhm, J. Bogusz, M. Bos, E. Brockmann, M. Cadeddu, B. Chimani, J. Douša, G. Elgered, M. Eliaš, R. Fernandes, M. Figurski, E. Fionda, M. Gruszczynska, G. Guerova, J. Guijarro, C. Hackman, R. Heinkelmann, J. Jones, S. Zengin Kazancı, A. Klos, D. Landskron, J. P. Martins, V. Mattioli, B. Mircheva, S. Nahmani, R. T. Nilsson, T. Ning, G. Nykiel, A. Parracho, E. Pottiaux, A. Ramos, P. Rebischung, A. Sá, W. Dorigo, H. Schuh, G. Stankunavicius, K. Stępniak, H. Valentim, R. Van Malderen, P. Viterbo, P. Willis and A. Xaver (2020). "Use of GNSS Tropospheric Products for Climate Monitoring (Working Group 3)". In: *Advanced GNSS Tropospheric Products for Monitoring Severe Weather Events and Climate*. Ed. by J. Jones et al. Springer Nature Switzerland AG. DOI: 10.1007/978-3-030-13901-8_5.

Bock, Olivier, Christian Keil, Evelyne Richard, Cyrille Flamant and Marie Noelle Bouin (2005). "Validation for precipitable water from ECMWF model analyses with GPS and radiosonde data during the MAP SOP". In: *Q. J. R. Meteorol. Soc.* 131.612, pp. 3013–3036. DOI: 10.1256/qj.05.27.

Dirksen, R. J., M. Sommer, F. J. Immler, D. F. Hurst, R. Kivi and H. Vömel (2014). "Reference quality upper-air measurements: GRUAN data processing for the Vaisala RS92 radiosonde". In: *Atmos. Meas. Tech.* 7.12, pp. 4463–4490. DOI: 10.5194/amt-7-4463-2014.

Held, Isaac M. and Brian J. Soden (2000). "Water Vapor Feedback and Global Warming". In: *Annu. Rev. Energy Environ.* 25, pp. 441–475.

Hicks-Jalali, Shannon, Robert J. Sica, Alexander Haefele, Giovanni Martucci, Eliane Maillard Barras and Jordan Voirin (2020). "A Raman Lidar Tropospheric Water Vapour Climatology and Height-Resolved Trend Analysis over Payerne Switzerland". In: *Atmos. Chem. Phys. Discuss.*, pp. 1–29. DOI: https://doi.org/10.5194/acp-2019-1089.

Hocke, Klemens, Leonie Bernet, Jonas Hagen, Axel Murk, Matthias Renker and Christian Mätzler (2019). "Diurnal cycle of short-term fluctuations of integrated water vapour above Switzerland". In: *Atmos. Chem. Phys.* 19.19, pp. 12083–12090. DOI: 10.5194/acp-19-12083-2019. URL: https://www.atmos-chem-phys.net/19/12083/2019/.

Möller, F. (1963). " On the influence of changes in the CO 2 concentration in air on the radiation balance of the Earth's surface and on the climate ". In: *J. Geophys. Res.* 68.13, pp. 3877–3886. DOI: 10.1029/jz068i013p03877.

Morland, J., Collaud M. Coen, Klemens Hocke, P. Jeannet and C. Mätzler (2009). "Tropospheric water vapour above Switzerland over the last 12 years". In: *Atmos. Chem. Phys.* 9.16, pp. 5975–5988. DOI: 10.5194/acp-9-5975-2009.

Nilsson, T. and G. Elgered (2008). "Long-term trends in the atmospheric water vapor content estimated from ground-based GPS data". In: *J. Geophys. Res. Atmos.* 113.19. DOI: 10.1029/2008JD010110.

Ning, T., J. Wang, G. Elgered, G. Dick, J. Wickert, M. Bradke, M. Sommer, R. Querel and D. Smale (2016). "The uncertainty of the atmospheric integrated water vapour estimated from GNSS observations". In: *Atmos. Meas. Tech.* 9.1, pp. 79–92. DOI: 10.5194/amt-9-79-2016.

Nyeki, Stephan, Stefan Wacker, Christine Aebi, Julian Gröbner, Giovanni Martucci and Laurent Vuilleumier (2019). "Trends in surface radiation and cloud radiative effect at four Swiss sites for the 1996–2015 period". In: *Atmos. Chem. Phys.* 19.20, pp. 13227–13241. DOI: 10.5194/acp-19-13227-2019.

Parracho, Ana C., Olivier Bock and Sophie Bastin (2018). “Global IWV trends and variability in atmospheric reanalyses and GPS observations”. In: *Atmos. Chem. Phys.* 18.22, pp. 16213–16237. DOI: 10.5194/acp-18-16213-2018.

Peng, Wang, Xie Tongchuan, Dai Jiageng, Sun Jingmin, Wu Yanling, Song Qingli, Dai Xin, Yuan Hongliang, Song Dejun and Zhao Jinrong (2017). “Trends and Variability in Precipitable Water Vapor throughout North China from 1979 to 2015”. In: *Adv. Meteorol.* 2017, pp. 1–10. DOI: 10.1155/2017/7804823.

Schneider, M., P. M. Romero, F. Hase, T. Blumenstock, E. Cuevas and R. Ramos (2010). “Continuous quality assessment of atmospheric water vapour measurement techniques: FTIR, Cimel, MFRSR, GPS, and Vaisala RS92”. In: *Atmos. Meas. Tech.* 3.2, pp. 323–338. DOI: 10.5194/amt-3-323-2010.

Trends of atmospheric water vapour in Switzerland from ground-based radiometry, FTIR and GNSS data

Leonie Bernet[1,2], Elmar Brockmann[3], Thomas von Clarmann[4], Niklaus Kämpfer[1,2], Emmanuel Mahieu[5], Christian Mätzler[1,2], Gunter Stober[1,2], and Klemens Hocke[1,2]

[1]Institute of Applied Physics, University of Bern, Bern, Switzerland
[2]Oeschger Centre for Climate Change Research, University of Bern, Bern, Switzerland
[3]Federal Office of Topography, swisstopo, Wabern, Switzerland
[4]Institute of Meteorology and Climate Research, Karlsruhe Institute of Technology, Karlsruhe, Germany
[5]Institute of Astrophysics and Geophysics, University of Liège, Liège, Belgium

Correspondence: Leonie Bernet (leonie.bernet@iap.unibe.ch)

Abstract.

Vertically integrated water vapour (IWV) is expected to increase globally in a warming climate. To determine whether IWV increases as expected on a regional scale, we present IWV trends in Switzerland from ground-based remote sensing techniques and reanalysis models, considering data for the time period 1995 to 2018. We estimate IWV trends from a ground-based microwave radiometer in Bern, from a Fourier Transform Infrared (FTIR) spectrometer at Jungfraujoch, from reanalysis data (ERA5 and MERRA-2) and from Swiss ground-based Global Navigation Satellite System (GNSS) stations. Using a straightforward trend method, we account for jumps in the GNSS data, which are highly sensitive to instrumental changes. We found that IWV generally increased by 2 to 5 % per decade, with deviating trends at some GNSS stations. Trends were significantly positive at ~~23 %~~ 17 % of all GNSS stations, which often lie at higher altitudes (between 850 and ~~1700 m~~ 1650 m above sea level). Our results further show that IWV in Bern scales to air temperature as expected (except in winter), but the IWV–temperature relation based on reanalysis data in whole Switzerland is not everywhere clear. In addition to our positive IWV trends, we found that the radiometer in Bern agrees within 5 % with GNSS and reanalyses. At the high altitude station Jungfraujoch, we found a mean difference of 0.26 mm (15 %) between the FTIR and coincident GNSS data, improving to 4 % after an antenna update in 2016. In general, we showed that ground-based GNSS data are highly valuable for climate monitoring, given that the data have been homogeneously reprocessed and that instrumental changes are accounted for. We found a response of IWV to rising temperature in Switzerland, which is relevant for projected changes in local cloud and precipitation processes.

1 Introduction

Atmospheric water vapour is a key component in the climate system. It is the most abundant greenhouse gas and responsible for a strong positive feedback that enhances temperature increase induced by other greenhouse gases (e.g. IPCC, 2013; Stocker et al., 2001). Furthermore, water vapour is involved in important tropospheric processes such as cloud formation ~~, it builds~~

~~the link between temperature~~ and precipitation, it influences size, composition and optical properties of aerosols and it is responsible for atmospheric energy and heat transport via evaporation and condensation (Kämpfer, 2013). Measuring changes in atmospheric water vapour is thus important because they reflect externally forced temperature changes in the climate system and can be an indicator for changes in involved processes such as cloud formation and precipitation. Concentrating hereby on regional changes is of special interest, because water vapour is spatially variable and the relation between water vapour, temperature and precipitation shows spatial dependencies.

Temperature and water vapour are closely linked as expected from the Clausius-Clapeyron relation. Several studies have revealed spatial correlation between mass changes of vertically integrated water vapour (IWV) and changes in temperature, especially over oceans (e.g. Wentz and Schabel, 2000; Trenberth et al., 2005; Wang et al., 2016). Nevertheless, it has also been shown that water vapour scales not everywhere to temperature as expected and that large regional differences exist (e.g. O'Gorman and Muller, 2010; Chen and Liu, 2016; Wang et al., 2016). Over continental areas, correlations between surface temperature and IWV changes are smaller than over oceans, showing in some regions even opposite trends (Wagner et al., 2006). Also, temperature climate feedbacks may have regional dependencies (Armour et al., 2013). Regional analyses of changes in water vapour and the relation to temperature changes are thus required.

Most of the atmospheric water vapour resides in the troposphere. Measuring IWV, vertically integrated over the whole atmospheric column, is therefore representative for tropospheric water vapour. The IWV can be measured by different techniques. Nadir sounding satellite techniques provide global data sets of IWV that have been used for global trend analyses in multiple studies (e.g. Trenberth et al., 2005; Santer et al., 2007; Wentz et al., 2007; Mieruch et al., 2008; Hartmann et al., 2013; Ho et al., 2018; Zhang et al., 2018). Most of these studies found global IWV trends between 1 and 2 % per decade, with large spatial differences. However, these satellite data sets have some limitations for regional IWV trend analyses. First, missing homogenization across multiple satellite platforms can make satellite trend studies difficult (Hartmann et al., 2013; John et al., 2011). Second, ~~many satellite products~~ visible and infrared satellite techniques are limited to clear-sky measurements. Further, satellite products from passive mircowave sensors are restricted to oceans only, because the well-known ocean surface emissivity makes retrievals generally easier over oceans than over land surfaces (Urban, 2013). Stable and long-term station measurements from ground are therefore more appropriate for regional IWV trend analyses over land. From ground, IWV can be measured by radiosondes (Ross and Elliot, 2001), sun photometers (Precision Filter Radiometers (PFR), Ingold et al. (2000), Wehrli (2000)), Fourier transform infrared (FTIR) spectrometers (Sussmann et al., 2009; Schneider et al., 2012), or microwave radiometers (Morland et al., 2009). Radiosondes ~~probably~~ provide the longest time series, but the homogeneity of the records can be problematic due to changes in instrumentation or observational routines (Ross and Elliot, 2001) and the temporal sampling is sparse (usually twice a day). PFR and FTIR instruments measure during day and clear-sky conditions only, whereas microwave radiometers can measure in almost all weather conditions during day and night with high temporal resolution. However, no dense measurement network exist for these techniques. Another technique that provides data in all weather situations are ground-based receivers of the Global Navigation Satellite System (GNSS). The advantage of GNSS receivers is the high spatial resolution due to dense networks. In the present study we combine the microwave and FTIR techniques at two Swiss measurement stations with data from the ground-based GNSS network in Switzerland to analyse IWV trends.

Several studies use GNSS measurements to derive global IWV trends over land (e.g. Chen and Liu, 2016; Wang et al., 2016; Parracho et al., 2018). Chen and Liu (2016) report GNSS derived IWV trends at mid-latitudes of $1.46\,\%$ per decade, and Parracho et al. (2018) found IWV trends in the northern hemisphere of approximately $2.6\,\%$ per decade based on GNSS and reanalysis data. The high spatial resolution of some regional GNSS networks makes them a valuable data set for regional trend analyses of IWV. For Europe, IWV trends based on GNSS data have been presented, for example, for Germany (Alshawaf et al., 2017) and Scandinavia (Nilsson and Elgered, 2008), who observed large trend variability between different stations.

To the best of our knowledge, no regional analysis of IWV trends covering the whole area of Switzerland has been published so far. Some studies presented IWV trends at single Swiss stations (Morland et al., 2009; Sussmann et al., 2009; Hocke et al., 2011, 2016; Nyeki et al., 2019), but most of them cover shorter time periods than available today. Morland et al. (2009) and Hocke et al. (2011, 2016) presented IWV trends at Bern using the same microwave radiometer that we use in the present study. However, they use time series of maximal 13 years, whereas a time series of 24 years (1995-2018) is available now. Granted that Switzerland experienced strong warming in the last decade, an update is of particular interest. Indeed, nine of the warmest ten years in Switzerland (from 1864 to 2018) have occurred in the last two decades, and six of them lie in the last decade (NCCS, 2018). A recent study by Nyeki et al. (2019) presents GNSS based trends for longer time series (until 2015), but they concentrate only on four Swiss stations. In fact, none of the mentioned studies presents IWV trends in whole Switzerland.

Our study presents a complete trend analysis of IWV in Switzerland based on data from the Swiss GNSS station network, a microwave radiometer located in Bern, an FTIR spectrometer located at Jungfraujoch and from reanalysis models. We present IWV trends for time series of 24 years (radiometer, FTIR and reanalyses) or 19 years (GNSS) and analyse how they are related to observed changes in temperature. To avoid artificial trends, homogenized radiometer data have been used in the present study (Morland et al., 2009; Hocke et al., 2011). For the GNSS data, possible jumps due to instrumental changes have been considered in the trend analysis by using the feature of bias fitting in the trend programme of von Clarmann et al. (2010). The goal of our study is to present trends of IWV in Switzerland, to detect potential regional differences and to verify if water vapour increases as expected from the observed temperature rise.

2 Water vapour data sets

We compare IWV data from a microwave radiometer located in Bern and an FTIR spectrometer at Jungfraujoch with Swiss GNSS ground stations and reanalysis data (ERA5 and ~~MERRA2~~MERRA-2). Radiometer data are available from 1995 onwards. We therefore define our study period from January 1995 to December 2018, even though GNSS data are available only after 2000 (see Table 1). IWV is often given as the total mass of water vapour per square metre ($\mathrm{kg\,m^{-2}}$). However, we provide IWV data in mm, taking the density of water into account, which is often referred to as "total precipitable water vapour". Evidently not all of the water vapour is actually precipitable. To avoid confusion, we prefer the term integrated water vapour (IWV) and provide the amount in the more convenient unit of mm, where $1\,\mathrm{mm}$ corresponds to $1\,\mathrm{kg\,m^{-2}}$.

2.1 Microwave radiometer

The Tropospheric Water Radiometer (TROWARA) is a microwave radiometer that has been retrieving IWV and integrated liquid water (ILW) since November 1994 in Bern, Switzerland (46.95° N, 7.44° E, 575 m above sea level (a.s.l.)). It measures the thermal ~~emission lines of water vapour at~~ microwave emission at the frequencies 21.39 GHz, 22.24 GHz and 31.5 GHz with a time resolution of several seconds and an elevation angle of 40°. The measured signal is used to infer the atmospheric opacity, using the Rayleigh-Jeans approximation of the radiative transfer equation as described in Mätzler and Morland (2009) and Ingold et al. (1998).

The opacity linearly depends on the water content in the atmosphere, and can therefore be used to derive IWV and ILW (Mätzler and Morland, 2009; Hocke et al., 2017):

$$\tau_i = a_i + b_i IWV + c_i ILW, \tag{1}$$

where τ_i is the opacity of the i-th frequency channel of the radiometer. The coefficients a_i and b_i are statistically derived from nearby radiosonde measurements and fine-tuned with clear-sky measurements (Mätzler and Morland, 2009). The coefficient c_i is the Rayleigh mass absorption coefficient of liquid water.

The initial instrument setup and measurement principle is presented in Peter and Kämpfer (1992). To improve the measurement stability and data availability, the instrument was upgraded in 2002 and 2004 and a new radiometer model was developed (Morland, 2002; Morland et al., 2006). Further, it was moved into an indoor laboratory in November 2002, which made it possible to measure IWV even during light rain conditions (Morland, 2002). However, to maintain consistency with the measurements before 2002, data observed during rainy conditions were excluded in the present study as soon as the ILW exceeds 0.5 mm or rain is detected by the collocated weather station (Morland et al., 2009). We use hourly IWV data from the STARTWAVE database (http://www.iapmw.unibe.ch/research/projects/STARTWAVE/) which were derived from the opacities at 21.39 GHz and 31.5 GHz. TROWARA data before 2008 were harmonized (Morland et al., 2009) and data gaps ~~before 2009~~ were filled with data derived from a collocated radiometer as described by Hocke et al. (2011) and Gerber (2009).

2.2 Fourier transform infrared spectrometer

A ground-based solar Fourier transform infrared (FTIR) spectrometer is located at the high altitude observatory Jungfraujoch in Switzerland (46.55° N, 7.98° E, 3580 m a.s.l.). Water vapour information is retrieved from absorption in the solar spectrum at three spectral intervals within 11.7 and 11.9 µm. The optimized IWV retrieval for FTIR spectrometry is described by Sussmann et al. (2009) and instrumental details are given in Zander et al. (2008). FTIR measurements at Jungfraujoch provide water vapour data since 1984. For consistency with our study period, we use data only from 1995 to 2018. In this period, two FTIR instruments were installed at Jungfraujoch, with overlapping measurements from 1995 to 2001. Sussmann et al. showed that the bias between both instruments is negligible. We therefore compute monthly means of a merged time series including both instruments. FTIR measurements are weather dependent (cloud-free conditions are required) and provide thus irregularly sampled data at Jungfraujoch, with on average eight measurement days per month in our study period. This sparse sampling can be problematic when calculating monthly means. We therefore apply the resampling method proposed by Wilhelm et al. (2019) when calculating monthly means of FTIR derived IWV. For this, the background IWV data are determined by fitting a seasonal model to daily IWV means. The seasonal model is given by a mean IWV_0, the first two seasonal harmonics with periods $T_n = 365.25/n$ and the fit coefficients a_n and b_n:

$$IWV(t) = IWV_0 + \sum_{n=1}^{2} \left(a_n \cdot \sin\left(\frac{2\pi}{T_n} \cdot t\right) + b_n \cdot \cos\left(\frac{2\pi}{T_n} \cdot t\right)\right). \tag{2}$$

This seasonal model is fitted to the 15th of each month using a window length of 2 years. Due to the sparsity of the FTIR data, the model fit to each month provides a more robust estimate compared to the statistical monthly means, which might be based on only one or two days of observations at the beginning or end of a month that are not necessarily representative as a monthly mean. The measurement uncertainties of the obtained monthly mean values are derived from the covariance matrix of the model fit. Further, we also tested a seasonal model with higher seasonal harmonics. However, due to the sparse FTIR measurements it appeared not to be useful to improve the obtained monthly mean IWV estimates.

2.3 GNSS ground stations

The signal of GNSS satellites is delayed when passing through the atmosphere. This so called zenith total delay (ZTD) can be used to infer information about the atmospheric water vapour content. Various studies explain the method to derive IWV from the measured ZTD (e.g. Bevis et al., 1992; Hagemann et al., 2002; Guerova et al., 2003; Heise et al., 2009). We briefly summarize the procedure that we used in our study. The ZTD can be written as the sum of the zenith hydrostatic delay (ZHD) due to refraction by the dry atmosphere, and the zenith wet delay (ZWD) due to refraction by water vapour (Davis et al., 1985):

$$ZTD = ZHD + ZWD \tag{3}$$

The ZHD (in metres) is calculated from the surface pressure at each GNSS station as proposed by Elgered et al. (1991):

$$ZHD = (2.2768 \pm 0.024) \times 10^{-3} \frac{p_s}{f(\lambda, H)} \tag{4}$$

with surface pressure p_s in hPa. The dependency of the gravitational acceleration on latitude and altitude is considered in the function f (Saastamoinen, 1972):

$$f(\lambda, H) = 1 - 0.00266 \cos(2\frac{\lambda\pi}{180}) - 0.00028\,H \tag{5}$$

where λ is the station latitude in degrees and H is the station altitude in km. With the measured ZTD and the calculated ZHD, we obtain the ZWD (Eq. 3), which can then be used to infer information about the IWV in mm. It is calculated according to Bevis et al. (1992) with

$$IWV = \kappa\, ZWD \frac{1}{\rho_{H_2O}} \tag{6}$$

where ρ_{H_2O} is the density of liquid water ($\rho_{H_2O} = 1000\,\mathrm{kg\,m^{-3}}$). The factor κ is given by

$$\frac{1}{\kappa} = R_v\,(\frac{k_3}{T_m} + k_2')\,10^{-6} \tag{7}$$

with the constants k_3 and k_2' as derived by Davis et al. (1985) from Thayer (1974) ($k_3 = (3.776 \pm 0.004) \times 10^5\,\mathrm{K^2\,hPa^{-1}}$ and $k_2' = 17 \pm 10\,\mathrm{K\,hPa^{-1}}$). The required estimate of the mean atmospheric temperature T_m is linearly approximated from the surface temperature T_s (damped with the daily mean) as proposed by Bevis et al. (1992) ($T_m = 70.2\,\mathrm{K} + 0.72\,T_s$). The pressure p_s and the surface temperature T_s at the GNSS station are interpolated from pressure and temperature measurements at the closest meteorological station, assuming hydrostatic equilibrium and an adiabatic lapse rate of $6.5\,\mathrm{K\,km^{-1}}$.

We use hourly ZTD data from the Automated GNSS Network for Switzerland (AGNES), containing 41 antennas (at 31 locations), as well as data from a few stations that are part of the COGEAR network (https://mpg.igp.ethz.ch/research/geomonitoring/cogear-gnss-monitoring.html) and from two additional stations in Bern. The AGNES network has been established in 2001 (Schneider et al., 2000; Brockmann, 2001; Brockmann et al., 2001a, b) and it is maintained by the Swiss Federal Office of topography (swisstopo). A monitor web page shows the current status of all stations (AGNES swisstopo). In 2008, most of the antennas and receivers were enhanced from GPS only to GPS and GLONASS (Russian global navigation satellite system). Since spring 2015, AGNES has been a multi-GNSS network (Brockmann et al., 2016), using data also from Galileo (European global navigation satellite system) and BeiDou (Chinese navigation satellite system). All European GNSS data were reprocessed in 2014 within the second EUREF (International Association of Geodesy Reference Frame Sub-Commission for Europe) Permanent Network (EPN) reprocessing campaign as described in Pacione et al. (2017). In the present study, only the reprocessed ZTD products of swisstopo are used (Brockmann, 2015).

The stations used in our study are shown in Fig. 1 and listed in Table 1. We only use stations that provide measurements for more than 10 years. At some GNSS stations, a new antenna and receiver were installed at the same or nearby location, replacing the older ones after an overlapping measurement period. An antenna change often leads to a small height difference, which can lead to a jump in the ZTD time series. It is therefore important to decide how to handle such instrumental changes for trend analyses. In case of antenna and receiver replacements, we merged these stations to a single time series by calculating the mean value for overlapping periods. They are marked by "_M" (for "merged") in their station abbreviation (Table 1) and a potential jump was considered in the trend estimation (see Sect. 3.1). At nine stations, new multi-GNSS receivers and antennas were installed at an additional location near-by, but the old GPS-only receivers and antennas are still operating. Swisstopo installed such twin stations to ensure a best possible long-term consistency. Simply replacing antennas at all stations would not guarantee continuous time-series, even if the phase centers of the antennas are individually calibrated. Further, no calibrations are available for the tracked satellite systems Galileo and BeiDou until today. In the case of twin stations, we only used the old, continuous GPS-only station, because the stability is better suited for trend calculations than merged time series with potential data jumps.

2.4 Reanalysis data

IWV, relative humidity (RH) and temperature data from two reanalysis products are used in the present study, the ERA5 and the MERRA-2 reanalyses. The Modern-Era Retrospective Analysis for Research and Applications, version 2 (MERRA-2) is an atmospheric reanalysis from NASA's Global Modeling and Assimilation Office (GMAO), described in Gelaro et al. (2017). The MERRA-2 product used in the present study for IWV data contains monthly means of vertically integrated values of water vapour (GMAO, 2015a). The product used for temperature provides monthly mean profiles (GMAO, 2015b). Both MERRA-2 products have a grid resolution of $0.5\,^\circ$ latitude $\times$ $0.625\,^\circ$ longitude. The ERA5 reanalysis is the latest atmospheric reanalysis from the European Centre for Medium Range Weather Forecasts (ECMWF) (Hersbach et al., 2018). In the present study, we use an ERA5 product providing integrated water vapour (Copernicus CDS, a) and another product providing RH and temperature profiles (Copernicus CDS, b), both with a grid resolution of $0.25\,^\circ$ latitude $\times$ $0.25\,^\circ$ longitude (Copernicus Climate Change Service (C3S), 2017). Reanalysis models assume a smooth topography, that can deviate from the real topography, especially in mountainous regions (Bock et al., 2005; Bock and Parracho, 2019). For validation of reanalysis data with specific station data (e.g. GNSS), the reanalysis IWV value would need to be corrected for altitude differences as for example proposed by Bock et al. (2005) or Parracho et al. (2018). For linear trends, however, such a linear correction is not relevant. We therefore use uncorrected reanalysis data, which might lead to some differences in IWV when comparing reanalysis IWV directly with IWV measured from the radiometer or at a GNSS station.

When using reanalysis data for trend estimates, one has to keep in mind their limitations. Due to changes in observing systems of the assimilated data, the use of reanalyses for trend studies has been debated (e.g. Bengtsson et al., 2004; Sherwood et al., 2010; . The recent reanalysis products contain some improvements in handling possible steps in assimilated data. For example, the bias correction of assimilated data in ERA5 has been extended to more observation systems (Hersbach et al., 2018) and MERRA-2 reduced certain biases in water cycle data (Gelaro et al., 2017). Nevertheless, future studies have to assess whether these improvements affect the reliability of reanalysis data for trend estimates.

3 Methodology

We used a multilinear parametric trend model from von Clarmann et al. (2010) to fit monthly means of IWV to the following regression function:

$$y(t) = a + b\cdot t + \sum_{n=1}^{4}\left(c_n \cdot \sin\left(\frac{2\pi t}{l_n}\frac{2\pi}{l_n}\cdot t\right) + d_n \cdot \cos\left(\frac{2\pi t}{l_n}\frac{2\pi}{l_n}\cdot t\right)\right) \tag{8}$$

with the estimated IWV time series $y(t)$, the time vector of monthly means t, and the fit coefficients a to d. We account for annual ($l_1 = 12$ months) and semi-annual ($l_2 = 6$ months) oscillations, as well as for two additional overtones of the annual cycle ($l_3 = 4$ months and $l_4 = 3$ months). For the FTIR trends, the solar activity is additionally fitted by using F10.7 solar flux data measured at a wavelength of $10.7\,\mathrm{cm}$ (National Research Council of Canada). Uncertainties of the time series $y(t)$ are considered in a full error covariance matrix $\mathbf{S_y}$. As ~~uncertainties~~monthly uncertainties σ_{mon}, we use for TROWARA and GNSS data

$$\sigma_{mon} = \sqrt{\sigma_{\bar{x}}^2 + \sigma_{sys}^2}, \quad (9)$$

where σ_{sys} is a systematic error and $\sigma_{\bar{x}}$ is the standard error of the monthly mean~~$\sigma_{\bar{x}} = \sigma n^{-\frac{1}{2}}$ (with standard deviation~~, given by

$$\sigma_{\bar{x}} = \sigma n^{-\frac{1}{2}}, \quad (10)$$

with the standard deviation of the monthly mean σ and the number of measurements per month n~~)~~. The systematic error σ_{sys} is estimated to be 1 mm for TROWARA and 0.7 mm for GNSS data. ~~FTIR uncertainties~~ These values are based on results from Ning et al. (2016a), who assessed IWV uncertainties from a radiometer and GNSS observations in Sweden. Our monthly uncertainties used for TROWARA and GNSS are on average 8 % for TROWARA and around 5 % for a typical GNSS station. FTIR uncertainties (around 25 %) are based on the model fit of daily means as described in Sect. 2.2. For reanalysis data, we use a monthly uncertainty of 10%. This value has been chosen, because it is slightly larger than the mean relative difference of reanalysis data and TROWARA data at Bern (≈5 %). Further, it corresponds to the variability proposed by Parracho et al. (2018) for ERA-Interim and MERRA-2 that is due to model and assimilation differences. In addition to IWV trends, we determine reanalysis trends of RH (ERA5) and temperature (ERA5 and MERRA-2). We use monthly uncertainties of 10% to estimate RH trends, whereas the standard error of each averaged temperature profile (below 500 hPa) is used as monthly temperature uncertainties (around 2.5 K).

We generally express trends in percent per decade that are derived from the regression model output in mm per decade by dividing it for each data set by its mean IWV value of the whole period. A trend is declared to be significantly different from zero at 95 % confidence interval as soon as its absolute value exceeds twice its uncertainty.

3.1 Bias fitting in the trend model

The trend model is able to consider jumps in the time series, by assuming a bias for a given subset of the data. For this, a fully correlated block is added to the part of $\mathbf{S_y}$ that corresponds to the biased subset. For each subset, the block in $\mathbf{S_y}$ is set to the square of the estimated bias uncertainty of this block. This possibility of bias fitting in the trend estimation has been presented in von Clarmann et al. (2010) and is mathematically explained in von Clarmann et al. (2001). The method has been applied for example by Eckert et al. (2014) to consider a data jump after retrieval changes in a satellite product. It is also described in Bernet et al. (2019), in which it has been applied on ozone data to consider data irregularities in a time series due to instrumental anomalies.

The approach is illustrated with an exemplary case (Fig. 2). We used an artificial time series with a trend of 0.5 mm per decade, and added three change points with a constant bias for each subset. The change points represent for example an instrumental update, that leads to a constant bias in the following data. The biased time series has a trend of 1.19 ± 0.06 mm per decade, which is too large compared to the true trend of 0.5 ± 0.06 mm per decade. To improve the trend estimate, we add a fully correlated block in S_y for each biased subset, assuming a bias uncertainty of 5 %. We obtain a corrected trend of

$0.52 \pm 0.17\,\mathrm{mm}$, which corresponds within its uncertainties to the true trend of the unbiased time series. This demonstrates that the approach can reconstruct the true trend from a biased time series, with slightly increased trend uncertainties.

3.1.1 Bias fitting for GNSS trends

In the present study, we use the bias fitting on GNSS data sets to account for instrumental changes. Analysing IWV trends from GNSS data is challenging, because the measurements are highly sensitive to changes in the setup (mainly concerning antennas and radomes, but also receivers and cables) or in the environment (Pacione et al., 2017). The presented method is a straightforward way to obtain reliable IWV trend estimates despite possible data jumps due to instrumental changes. We consider each instrumental change in the trend programme, requiring as single information the dates when changes have been performed at the GNSS stations and an estimate of the bias uncertainty. We introduced change points in the trend programme as soon as ~~antenna updates have led to a~~ a possible jump in the GNSS data ~~, as~~ has been recorded by swisstopo (available at http://pnac.swisstopo.admin.ch/restxt/pnac_sta.txt)~~.~~ , which is mostly due to antenna updates.

After such antenna changes, we assume a bias uncertainty of 5% of the averaged IWV value for each biased subset. The bias uncertainty of 5 % has been chosen based on our example case at Neuchâtel (Fig. 3), in which we observed a bias of 4 % after an antenna change~~of 4 %~~. This is also consistent with results from Gradinarsky et al. (2002) and Vey et al. (2009), who found IWV jumps of around $1\,\mathrm{mm}$ due to antenna changes or changes in the number of observations and the elevation cutoff angles. For a typical Swiss station with averaged IWV values of around $16\,\mathrm{mm}$, this corresponds to a bias of around 6 %. Ning et al. (2016b) found IWV biases due to GNSS antenna changes mostly between 0.2 and $1\,\mathrm{mm}$, which corresponds to a bias of 1 to 6 %, confirming our choice of 5 % bias uncertainty. In addition to the antenna updates, we added change points in the GNSS time series when a new antenna and receiver has been added to replace an older ~~receiver~~ system near-by (see Table 1). This can lead to larger biases, and we therefore assume a bias uncertainty of 10 % due to this data merging. For some antenna updates, jumps have been observed back to a data level of a previous period. These subsets have then been considered as unbiased to each other. Otherwise, we assumed the ~~data block before the first change~~ longest data block to be the unbiased reference block.

The trend programme and the bias correction are illustrated by an exemplary case of the GNSS station in Neuchâtel, Switzerland (Fig. 3). Figure 3a shows the monthly IWV time series of GNSS data in Neuchâtel with antenna updates in the years 2000, 2007, and 2015 (vertical red dotted lines). Figure 3b shows the deseasonalized anomalies of the IWV time series, divided by the overall mean value of each month, illustrating the interannual variability. The ~~data variability is linked to the antenna and receiver changes, with smaller variability and less negative anomalies for the antenna used~~ anomalies are less variable from 2007 to ~~2015.~~ 2012, but it is not clear whether this is related to the antenna update in 2007. Furthermore, the relative difference to ERA5 $((\mathrm{ERA5}-\mathrm{GNSS})/\mathrm{GNSS})$ reveals a data jump after the antenna change in 2015 (Fig. 3b). After this antenna change, the mean difference to ERA5 has been reduced, suggesting that the antenna update improved the measurements. The jump corresponds to a bias in IWV of $0.66\,\mathrm{mm}$ (4 %) compared to the data before the change. Such a jump can falsify the resulting trend. In the corrected trend fit, the trend model therefore accounts for possible biases for each antenna update. When the bias is considered in the trend model, the jump in the difference to ERA5 is reduced (Fig. 3~~c and d~~b). Further, we obtain a larger ~~trend ($0.78 \pm 0.84\,\mathrm{mm}$~~ bias corrected trend ($0.78 \pm 0.89\,\mathrm{mm}$ per decade) compared to the trend of the initial data

(~~$0.33 \pm 0.43\,\mathrm{mm}$~~ $0.33 \pm 0.44\,\mathrm{mm}$ per decade) ~~.~~ (Fig. 3c and d). In general, the trend fit (Fig. 3c) reproduces well the IWV time series. For both model fits, $90\,\%$ of the residuals (Fig. 3d) lie within $2\,\mathrm{mm}$, which corresponds to differences between observed data and model fit below ~~16~~17 %. The regression model explains 93% of the variability of the IWV time series at this station.

4 Integrated water vapour around Bern

IWV measurements from the TROWARA radiometer in Bern are compared to surrounding GNSS stations and reanalysis data. Figure 4 shows monthly means of TROWARA and reanalyses, as well as the averaged monthly means of seven GNSS stations close to Bern. The selected GNSS stations lie within $\pm 0.5°$ latitude and $\pm 1°$ longitude around Bern, with a maximal altitude difference of $200\,\mathrm{m}$ (see Table 1). The altitude restriction has been chosen to avoid the inclusion of the two higher altitude stations (Zimmerwald and Bourrignon), that are close to Bern but show larger IWV variability due to their higher elevation.

Generally, we observe a good agreement between the data sets, with interannual variability that is captured by all data sets (Fig. 4b). The data sets agree well with TROWARA, with averaged differences smaller than $0.6\,\mathrm{mm}$ ($\sim 5\,\%$). Only the stations in Bern (WAB1 and EXWI) show a bias compared to TROWARA (not shown). The Huttwil (HUTT) station reports less IWV than TROWARA, which is probably due to the higher station altitude. The GNSS stations around Bern agree well with TROWARA after 2013, and show larger winter differences before 2008 (Fig. 4c).

ERA5 agrees generally well with TROWARA, whereas MERRA-2 differs slightly more. Especially in the last decade, the MERRA-2 difference to TROWARA shows a strong seasonal behaviour with larger differences in winter, which is not visible in the other data sets. Correcting the reanalysis data for a possible altitude mismatch due to wrong topography assumptions (Bock and Parracho, 2019) might partly reduce discrepancies between reanalyses and observations.

4.1 IWV trends around Bern

Trends of IWV for the different data sets around Bern are shown in Fig. 5 and Table 2. IWV measured by the radiometer TROWARA increased significantly by $4.8\,\%$ per decade from 1995 to 2018. This trend value is similar to the ~~observed~~ bias corrected trends from GNSS stations in Lausanne (EPFL), Huttwil (HUTT), Luzern (LUZE), Neuchâtel (NEUC) and Wabern next to Bern (WAB1), which all report trends around $5\,\%$ per decade (Fig. 5 and Table 2). We observe a slightly ~~smaller trend in Luzern (LUZE, $3.6\,\%$ per decade) and a~~ larger trend in Payerne (PAYE, ~~$7.3\,\%$~~ $7.0\,\%$ per decade). The GNSS station in Bern, located at the roof of the University building of exact sciences (EXWI), shows a trend of quasi zero ($0.1\,\%$ per decade). Unfortunately, the site EXWI is no longer in operation since Sept. 2017. ~~With the exception of Payerne, all these GNSS trends are not significantly different from zero at 95% confidence interval.~~ Reanalysis IWV at Bern increases significantly by $3.7\,\%$ per decade for MERRA-2 and by $2.3\,\%$ per decade for ERA5 data~~. However, the uncertainties of the monthly reanalysis data might be larger than the here used value of 10%~~ ~~, which would also lead~~ both for the period from 1995 to ~~larger uncertainties of the reanalysis trends .~~ 2018. With the exception of Payerne, all GNSS trends are not significantly different from zero at 95% confidence interval. The larger GNSS trend uncertainties compared to TROWARA and reanalysis trends are mainly due to the bias correction, which adds some uncertainty to the trend estimates. Further, all GNSS trends result from a shorter time period than TROWARA and reanalysis trends (see Table 1), which also increases the trend uncertainty and may lead to some trend differences. For comparison, the GNSS trends without bias correction are also shown in Table 2. They are generally smaller than the bias corrected trends, suggesting that GNSS trends are mostly underestimated when biases are not accounted for. Further, their uncertainties are smaller, reflecting the additional uncertainty when biases are considered.

In brief, most of the GNSS stations around Bern report positive trends of approximately 5 % per decade~~(0.9 mm per decade)~~. However, two of the GNSS stations around Bern (EXWI and PAYE) report different trends. The quasi zero trend at the EXWI station is less reliable than the other trends, because the EXWI station ~~provides data in a shorter time period (until 2016). Further, it~~ is not part of the AGNES network and therefore does not fulfil the same quality requirements. The large GNSS trend in Payerne results from the bias correction. If the bias correction in the trend fit (as described in Sect. 3) is not applied, the trend in Payerne is only 2 % per decade (0.32 mm per decade), whereas it increases to ~~7.3 %~~ 7.0 % per decade (~~1.14 mm~~ 1.09 mm per decade) when accounting for antenna changes. Nyeki et al. (2019) found IWV trends in Payerne from GNSS measurements of 0.8 mm per decade, which lies between our corrected and uncorrected trends. It suggests that the instrumental changes in Payerne play an important role, but might be overcorrected in our case. The recent study of Hicks-Jalali et al. (2020) reports similar IWV trends in Payerne using nighttime radiosonde measurements (6.36 % per decade) and even larger trends using clear-night lidar data (8.85 % per decade) in the period from 2009 to 2019, suggesting that IWV in Payerne was strongly increasing, especially in recent years. However, comparing their trend results with ours has to be done with care, because their trend time period is short and the lidar trends might contain a clear-sky bias.

The trend from the TROWARA radiometer of 4.8 % per decade (0.72 mm per decade) slightly differs from the TROWARA trends reported by Morland et al. (2009) and Hocke et al. (2011, 2016). It is larger than TROWARA's 1996 to 2007 trend of 3.9 % per decade (0.56 mm per decade) (Morland et al., 2009). Hocke et al. (2011) found no significant TROWARA trend for the period 1994 to 2009, which suggests that our larger IWV trends are mainly due to a strong IWV increase in the last decade. This is also confirmed by Hocke et al. (2016), who observed larger trends for recent years (1.5 mm per decade for 2004 to 2015). However, care has to be taken when comparing these TROWARA trends of different trend period lengths.

To summarize, IWV trends around Bern from TROWARA and GNSS data generally lie around 5 % per decade, whereas reanalysis trends for the Bern grid are slightly smaller. ~~Some GNSS stations deviate from these trend values, probably due to instrumental issues.~~

4.1.1 Seasonal IWV trends around Bern

To study the seasonal differences of the IWV trends around Bern, we analysed trends for each month of the year (Fig. 6). The absolute trends (Fig. 6a) are largest in summer months due to more IWV in summer. The trends in percent (Fig. 6b) account for the seasonal cycle in IWV, leading to more uniform trends throughout the year. However, differences between winter trends might sometimes be overweighted when calculating trends in percent: A small trend difference in winter will be more important when expressed in percent than the same difference in summer trends, because of less water vapour in winter. Nevertheless, we will concentrate on trends in percent per decade in the following, which facilitates comparing ~~trends of~~ relative changes of IWV in different seasons.

Our monthly trends in Bern mostly agree on largest and significant trends in June ($\sim$7 to 9 % per decade) and in November ($\sim$8 to ~~9 %~~ 10 % per decade) and minimal, but insignificant trends in February and October (Fig. 6b). Further, all data sets report a special pattern of low trends in October, with again larger trends in November. ~~The mean GNSS trend~~ However, the differences between those monthly trends are significant only at 68% confidence level. The mean trend (arithmetic mean) of the GNSS stations around Bern agrees with the other data sets in summer, but shows an offset to the other trends in several months, especially in March and in autumn. ~~Most of the used GNSS stations are not located within the Bern reanalysis grid, which might explain some of the trend differences. The better agreement in summer suggests that the spatial difference is less critical in summer conditions.~~ We further found that MERRA-2 trends are slightly larger in summer than trends from the other data sets, whereas TROWARA trends differ from the other trends in the winter months December and January. This larger disagreement between TROWARA and reanalysis trends in December and January is consistent with the larger winter biases of TROWARA starting in 2008 in Fig. 4c.

Previous studies analysed TROWARA seasonal trends using shorter time periods. Morland et al. (2009) and Hocke et al. (2011) observed significant positive summer trends and negative winter trends for TROWARA. Our TROWARA trends confirm positive summer trends (significant in June and August), but do not confirm negative winter trends. The observed autumn peak (minimum trend in October and a trend peak in November) has also been reported by Morland et al. (2009) and Hocke et al. (2011). However, their trend peak was shifted by two months, with a minimum in August and a subsequent maximum in September. The ten additional years that we use in our study compared to their data might be responsible for this shift. Morland et al. (2009) proposed that this autumn trend peak might be related to precipitation changes, but such a relationship has not been verified for the present study. Nevertheless, we showed that the IWV trend peak is consistent with November temperature trends, suggesting that those trends are temperature driven (see Sect. 4.2 and Fig. 6c).

In summary, Bern data sets generally agree on the annual trend distribution, with largest trends in June and in November. However, the monthly trends of GNSS stations around Bern disagree with the other datasets in spring and in autumn, whereas TROWARA deviates in December and January. Positive summer trends are reported by all data sets.

4.2 Changes in IWV and temperature around Bern

To examine the relationship between IWV trends and changing temperature, we present the theoretical change of water vapour in the atmosphere due to observed changes in temperature (Fig. 6~~b~~c). For this, we determined the temperature dependent change in saturation vapour pressure for the time period 1995 to 2018. The saturation vapour pressure e_s describes the equilibrium pressure of water between the condensed and the vapour phase. It increases rapidly with increasing temperature (Held and Soden, 2000). In case that the water vapour pressure e is smaller than e_s, the available water ~~evaporates~~ is in vapour phase, whereas for ~~$e > e_s$ it condensesuntil it reaches the equilibrium ($e = e_s$)~~ $e \geq e_s$ it condenses. With increasing temperature, e_s increases, which leads for a given ~~e~~ relative humidity (RH) to an increase of ~~water vapour in the vapour phase~~ e. Changes in

e_s can therefore directly be compared to changes in the amount of water vapour ~~. A required assumption is that the relative humidity (RH) remains constant ,~~ assuming that RH remains constant (Möller, 1963; Held and Soden, 2000):

$$RH = \frac{e}{e_s} \approx \cancel{\text{constant}}\text{constant}. \tag{11}$$

~~so that a~~ A change in e_s is then directly reflected in a change in e, and therefore in IWV:

$$\frac{de_s}{e_s} \approx \frac{de}{e} = \frac{dIWV}{IWV}. \tag{12}$$

The fractional change of e_s for a given change in temperature can be approximated by the Clausius-Clapeyron equation:

$$\frac{de_s}{e_s} \approx \frac{L_v}{R_v T^2} dT, \tag{13}$$

where L_v is the latent heat of evaporation ($L_v = 2.5 \times 10^6\,\mathrm{J\,kg^{-1}}$), R_v is the gas constant for water vapour ($R_v = 461\,\mathrm{J\,K^{-1}\,kg^{-1}}$), dT is the change in temperature and T is the actual temperature. To obtain the tropospheric temperature change dT, we derived the temperature trend (1995 to 2018) from MERRA-2 and ERA5 temperature profiles, averaged below $500\,\mathrm{hPa}$. This limit was chosen because 95 % of IWV resides below $500\,\mathrm{hPa}$ for the averaged MERRA-2 profiles in our study period. The resulting temperature trend (in K per decade) is then used for dT in Eq. (13) to determine the change in e_s in percent per decade. For the actual temperature T we used the mean of reanalysis temperature profiles below $500\,\mathrm{hPa}$ for the same time period.

The fractional changes in ERA5 e_s for the Bern grid for different months are shown ~~by the grey lines~~ in Fig. 6~~b~~c. These temperature induced changes in e_s agree generally well with the observed trends in IWV. They agree especially well with TROWARA and reanalysis trends in spring (March and April), late summer and autumn (July to November), and less good in the winter months and in May and June. Furthermore, they agree less with GNSS trends from September to March~~, which might again partly be explained by the spatial difference of most GNSS stations to the used reanalysis grids at Bern~~. Generally, the good agreement between the change in e_s and the IWV trends indicates that observed IWV changes around Bern can mostly be explained by temperature changes. However, the changes in e_s do not confirm our observed IWV winter trends, especially in January and February. This discrepancy ~~might~~ can be related to ~~temperature inversions that are often present in winter. In these situations, the surface water vapour is trapped by the inversion and less propagating in the free troposphere (?), which means that the water vapour content does not scale anymore to temperature above the inversion layer~~changes in RH, which was assumed to be constant (Eq. (11)). Indeed, our trends of ERA5 RH for the Bern grid (Fig. 6c) show that RH was not constant in those months, especially in winter but also in May and June. Even though the RH trends are not significantly different from zero, these results suggest that assuming RH to be constant may not be valid during all seasons, especially in winter. This makes the attribution of IWV trends to changes in temperature more challenging. Furthermore, other factors than temperature might be responsible for IWV changes in winter, such as changes in dynamical patterns and the horizontal transport of humid air. Indeed, Hocke et al. (2019) showed that evaporation of surface water plays a minor role in winter, with a latent heat flux that is in Bern six to seven times smaller than in summer, suggesting that horizontal transport of humid air is in winter more important than evaporation. ~~We thus~~

We conclude that IWV in Bern changes as expected from temperature changes in early spring, late summer and autumn, but other processes might also be responsible for IWV changes, especially in winter.

5 Integrated water vapour at Jungfraujoch

We compare IWV at Jungfraujoch from a GNSS antenna and an FTIR spectrometer ~~.~~ (Fig. 7). Due to the sparser FTIR sampling, we compare FTIR data not only with the full GNSS time series, but also with coincident GNSS data, i.e. pairwise data limited to clear-sky weather conditions. Monthly means of these sparser data have been computed by a seasonal fitting as described in Sect. 2.2. This leads to some missing data at the edges of the coincident GNSS time series (Fig. 7a,c), because a specific number of data points is required for the seasonal fitting. For the FTIR time series, no data are missing at the edges because data were available beyond the dates of our study period.

We observe less IWV at Jungfraujoch than at Bern due to the high altitude of the station, with mean IWV from GNSS of $3\,\mathrm{mm}$ (Fig. 7a). The deseasonalised anomalies (Fig. 7b) show that the interannual variability of IWV at Jungfraujoch is larger than in Bern, with anomalies larger than $50\,\%$ for some months. ~~A mean bias of $-0.26 \pm 0.3\,\mathrm{mm}$ is found when comparing monthly~~ Monthly means of coincident GNSS ~~and FTIR measurements (~~data have a mean dry bias of $-0.26 \pm 0.3\,\mathrm{mm}$ compared to FTIR (GNSS$_{\mathrm{coincident}}$ – FTIR) (Fig. 7c). This corresponds to a bias of $15\,\%$ when referring to the long-term average of GNSS coincident IWV data. ~~Compared to the~~ Further, monthly means of fully sampled GNSS ~~time series, we found~~ have a bias of $1.05 \pm 0.61\,\mathrm{mm}$ compared to FTIR (GNSS – FTIR), which corresponds to a bias of $34\,\%$ (using the mean of the fully sampled GNSS as reference). This larger bias illustrates the sampling effect of the FTIR measurements, leading to a dry bias of FTIR compared to GNSS data. Indeed, the difference results from the restriction that FTIR measurements require clear-sky conditions, preventing measurements during the wettest days. ~~Nevertheless, the~~

The remaining bias of $-0.26\,\mathrm{mm}$ when using coincident GNSS measurements indicates that GNSS measures slightly less IWV than FTIR. This ~~result~~ is consistent with results from Schneider et al. (2010), who report that GNSS at the high altitude Izaña Observatory (Tenerife) systematically underestimates IWV in dry conditions ($< 3.5\,\mathrm{mm}$). Further, a dry bias has also been observed in previous studies that ~~reported negative GNSS biases compared to~~ compared Jungfraujoch GNSS data with Precision Filter Radiometer (PFR) data ~~at Jungfraujoch~~ (Guerova et al., 2003; Haefele et al., 2004; Nyeki et al., 2005; Morland et al., 2006). Guerova et al. attributed this bias to incorrect modelling of the antenna phase centre and Haefele et al. to unmodeled multi-path effects of the Jungfraujoch antenna. Brockmann et al. (2019) stated that the old GPS-only antenna used at Jungfraujoch till 2016 was never calibrated. Due to the special radome construction (with circulating warm air to avoid icing), the standard antenna phase center calibration is not appropriate to be used with the Jungfraujoch data. From this point of view the achieved results are ~~astonishingly good . For trend analyses, a possible offsets~~ good and a possible offset is not relevant for trend analyses as long as it is constant over the whole trend period. The use of this antenna was stopped in summer 2015 and it was replaced by a new ~~multi-GNNS~~ multi-GNSS antenna in October 2016 (Brockmann et al., 2016). Furthermore, the complete antenna-radome construction was individually calibrated for GPS and GLONASS signals (Galileo and BeiDou are assumed to be identical to GPS). We found that the bias to FTIR has been reduced to $-0.07\,\mathrm{mm} \pm 0.28$ (4 %) after the antenna change in 2016, suggesting that the GNSS antenna update improved the consistency of the measurements at Jungfraujoch.

5.1 IWV trends at Jungfraujoch

The IWV trends at the Jungfraujoch station from FTIR and fully sampled GNSS data are presented in Fig. 8. The GNSS antenna update has been considered in the trend estimate as described in Sect. ~~3.1~~3.1.1. We observe IWV trends of 0.08 mm per decade (~~2.8 %~~ 2.6 % per decade) for GNSS and 0.04 mm per decade (1.8 % per decade) for FTIR. However, both trends are insignificant. The difference between both trends ~~might~~ can partly be explained by the dry sampling bias of the FTIR spectrometer, that measures only during clear-sky day conditions. Indeed, the absolute GNSS trend is comparable with the FTIR trend when we use GNSS data coincident with FTIR measurements, with 0.05 mm per decade (not shown). Our IWV trends at Jungfraujoch are similar to the trend by Sussmann et al. (2009), who reported insignificant FTIR trends at the same station of 0.08 mm per decade in the time period 1996 to 2008. In contrast to these results, Nyeki et al. (2019) found larger trends at Jungfraujoch that were significantly different from zero. They decided not to use GNSS IWV data from Jungfraujoch due to the high IWV variability and ~~problems due to the influence of snow and ice.~~ the missing calibration of the antenna before the replacement in 2016. Therefore, they derived their trends from IWV data based on a parameterisation from surface temperature and relative humidity measurements. However, they admit that this approximation is prone to large uncertainties (Gubler et al., 2012), which might explain parts of the differences to our trends.

6 IWV trends in Switzerland

6.1 Swiss GNSS trends

The GNSS data generally report positive IWV trends throughout Switzerland (Fig. 9). Using data for the whole year (Fig. 9a), 50 % of the stations show trends between ~~2.6 and 5.4 %~~ 2.3 and 5.1 % per decade (~~0.30 and 0.73 mm~~ 0.27 and 0.74 mm per decade). The trends of all stations range between 0.1 % per decade ~~(0.02 mm per decade) and 7.3 %~~ and 7.2 % per decade (~~1.14 mm per decade~~ 0.01 mm per decade and 1.09 mm per decade), with exception of three stations that show negative trends (ANDE, HOHT and MART_M). The mean trend value of all GNSS stations is ~~3.7 %~~ 3.6 % per decade (0.49 mm per decade) and the median is ~~4.0~~4.4 % per decade (0.57 mm per decade).

Only ~~four stations (11 %~~ three stations (9 % of all stations) show negative IWV trends and none of them is significantly different from zero at 95 % confidence interval. Significant positive trends are reported at ~~23~~17 % ~~percent~~ of the stations (~~eight~~ six stations), being generally stations with long time series and lying mostly in western and south eastern Switzerland. Most significant trends are observed in summer (Fig. 9d), with significant positive trends at five stations. In winter, only ~~the three~~ two north-eastern Swiss station trends are significant (Fig. 9b). In spring (Fig. 9c) and ~~autmun~~ autumn (Fig. 9e), none of the IWV trends are significantly different from zero. Autumn trends tend to be negative, especially in the southwestern part (Rhône valley in the canton of Valais), but they are all insignificant.

Our trend range covered by all GNSS stations is consistent with results from Nilsson and Elgered (2008), who observed in Sweden and Finland IWV trends between -0.2 and $1\,\mathrm{mm}$ per decade. However, they concluded that their study period was too short (10 years) to obtain stable trends. Our trends also lie within the range of trends observed in Germany by Alshawaf et al. (2017). Their trends vary even more between different stations, with trends ranging between -1.5 to $2.3\,\mathrm{mm}$ per decade. Note, however, that both studies use different trend periods lengths than in our study, which makes trend comparisons difficult. The recent study of Nyeki et al. (2019) reports IWV trends from GNSS data at three Swiss stations for the period 2001 to 2015. Using Sen's slope trend method, they found positive all-sky trends in Davos ($0.89\,\mathrm{mm}$ per decade), Locarno ($0.42\,\mathrm{mm}$ per decade) and Payerne ($0.80\,\mathrm{mm}$ per decade). Our GNSS trends for these stations are slightly different (Davos: $0.71\,\mathrm{mm}$ per decade, Locarno: ~~0.69 mm~~ $0.72\,\mathrm{mm}$ per decade, Payerne: ~~1.14 mm~~ $1.09\,\mathrm{mm}$ per decade), which might be due to the three additional years in our analysis, but also due to our bias correction in the trend model. Furthermore, our ~~GNSS~~ GNSS-derived ZTD data were reprocessed till 2014 (see Sect. 2.3), whereas Nyeki et al. still used the old ~~GNSS-derived ZTD~~ GNSS data.

The altitude dependence of the GNSS trends is shown in Fig. 10. We observe that most of the stations that show significant positive trends lie at higher altitudes~~(Fig. 10). Indeed, 88~~. Indeed, 83% of the stations ~~that show~~ showing significant trends lie at altitudes above $850\,\mathrm{m}$ a.s.l, whereas less than half of the stations lie above $850\,\mathrm{m}$. This is consistent with the expectation of Pepin et al. (2015) that the rate of warming is larger at higher altitudes. Due to the direct link between temperature and water vapour content, an increased warming at higher altitudes would lead to larger IWV trends. The increasing significance with altitude provides some observational evidence for this suggestion. However, the altitude dependence is less visible in absolute trends (not shown), which indicates that due to less IWV at higher altitudes, these trends are more sensitive to changes when calculating trends in percent. Also, the IWV trends of the ~~five~~ six stations with highest altitudes (~~$> 1700\,\mathrm{m}$~~ $> 1650\,\mathrm{m}$ a.s.l) are not significantly different from zero.

We conclude that Swiss GNSS stations generally show positive IWV trends, with a mean value of ~~3.4~~3.6 % per decade (~~0.44 mm~~ $0.49\,\mathrm{mm}$ per decade) and a tendency for more significant percentage trends at higher altitudes.

6.2 Swiss reanalysis trends

Reanalysis trends of IWV for Switzerland are presented in Fig. 11 and Fig. 12. The trends are on average $2.6\,\%$ per decade ($0.35\,\mathrm{mm}$ per decade) for ERA5 (Fig. 11a) and $3.6\,\%$ per decade ($0.52\,\mathrm{mm}$ per decade) for MERRA-2 (Fig. 12a). Both reanalysis trends show only small spatial variability. The seasonal trends are positive, with largest values in summer (Fig. 11d and 12d). This is consistent with our observed GNSS trends, which are mostly positive in summer. Smallest and partly negative reanalysis trends are observed in winter (Fig. 11b and 12b), which contrasts with our GNSS trends that showed smallest (but insignificant) trends in autumn and not in winter. In spring and autumn, the reanalysis trends are spatially more variable. Both data sets report slightly larger autumn trends in south-eastern Switzerland and northern Italy (Fig. 11e and 12e). 5 In spring, ERA5 shows larger IWV trends in south-western Switzerland.

~~Our mean ERA5 trend for Switzerland of 0.35 mm per decade is consistent with IWV trends from ERA-Interim in Germany reported by Alshawaf et al. (2017) (0.34 mm per decade). The~~ The averaged MERRA-2 ~~trends are generally slightly larger than the ERA5 trends. Parracho et al. (2018) also found larger IWV trends for MERRA-2 compared to ERA-Interim reanalysis~~

~~trends on a global scale, especially in summer. Our MERRA-2 trend (3.6 % per decade)~~ trend agrees with our averaged GNSS trend (~~3.4 %~~ both 3.6 % per decade), which is slightly larger than the averaged ERA5 trend (2.6 % per decade). However, the reanalyses do not resolve small scale variability, which can explain the differences to some GNSS station trends. Further, the GNSS point measurements are generally more variable than the gridded reanalyses data. Alshawaf et al. (2017) also observed larger differences in mountainous regions between GNSS derived IWV ~~trends and reanalyses~~ and reanalyses data in Germany. Our mean ERA5 trend for Switzerland of 0.35 mm per decade is consistent with IWV trends from ERA-Interim in Germany reported by Alshawaf et al. (2017) (0.34 mm per decade). The MERRA-2 trends are generally slightly larger than the ERA5 trends. Parracho et al. (2018) also found larger IWV trends for MERRA-2 compared to ERA-Interim reanalysis trends on a global scale, especially in summer.

To determine the relationship between temperature changes and IWV trends for whole Switzerland, we present changes in saturation vapour pressure e_s derived from reanalysis temperature changes below 500 hPa (as described in Sect. 4.2). The fractional change in e_s, which corresponds to the change in IWV (Eq. 12) is presented for ERA5 (Fig. 13) and for ~~MERRA-2~~ MERRA-2 (Fig. 14). The averaged changes in e_s of 2.9 % per decade (ERA5) and 4.0 % per decade (MERRA-2) are similar to our reanalysis IWV trends described before, which indicates that IWV is on average following the temperature change as expected from the Clausius-Clapeyron equation. The ERA5 e_s changes are spatially more uniform than the ERA5 IWV trends, but agree well in all seasons, except in winter (Fig. 13b and 11b). ~~This indicates~~ ERA5 e_s is decreasing in winter, whereas ERA5 IWV winter trends are increasing. These conflicting results indicate that other factors than temperature might dominate IWV changes in winter, as already discussed in Sect. 4.2. ~~In contrast to ERA5, The MERRA-2 changes in e_s show large spatial variability, with strong differences between different grids and generally larger values in the Alpine region. On regional scales, the MERRA-2 e_s~~ Further, it indicates that the assumption of constant relative humidity might not be valid in winter. This is confirmed by the ERA5 RH trends (Fig. ~~14)thus differ strongly from the MERRA-2 IWV trends (Fig. 12), especially in summer and~~ 15), which are around zero for whole Switzerland in all seasons but slightly positive in winter. Even though these positive winter RH trends are not significantly different from zero, they raise the question whether it is justified to assume RH to be constant.

The partly negative winter changes in e_s are surprising, because they result from a decrease in reanalysis winter temperature. Such a decrease in winter temperature is controversial to long-term temperature observations in Switzerland, that report a temperature increase also in winter (Begert and Frei, 2018). This difference is ~~probably~~ due to our short study period. A few cold winters in the past 15 years ~~might~~ have hidden the overall positive temperature trend when looking only at the relatively short period from 1995 to 2018 (MeteoSwiss, 2019).

In ~~general, we should be careful to draw conclusions from the reanalysis trends because of their uncertainties. Due to changes in observing systems of the assimilated data, the use of reanalyses for trend studies has been debated (e.g. Bengtsson et al., 2004; Sherwood et al., 2010; Dee et al., 2011; Parracho et al., 2018). This problem has been addressed in the recent reanalysis products. Compared to the previous ECMWF reanalysis (ERA-Interim), the bias correction of assimilated data in~~ contrast to ERA5~~has been extended to more observation systems (Hersbach et al., 2018). Also~~ , The MERRA-2 changes in e_s show large spatial variability, with strong differences between different grids and generally larger values in the Alpine region. These large values are caused by a jump in MERRA-2 ~~has been improved compared to the previous MERRA data , for example with reduced biases in the water cycle (Gelaro et al., 2017). Further analyses would be required to conclude if biases due to changes in observing systems still exist in the reanalysis data over Switzerland.~~ tropospheric temperature data around the year 2017 in the Alpine grids, which results in strong temperature trends. This might be due to MERRA-2 model changes in topography or assimilated data. In the Alpine region, the MERRA-2 changes in e_s (Fig. 14) thus differ strongly from the MERRA-2 IWV trends (Fig. 12).

To summarize, the reanalysis IWV trends follow on average the changes expected from temperature changes~~, but~~ . However MERRA-2 shows large regional variability for changes in e_s ~~based on~~ due to biases in lower tropospheric temperature ~~changes~~data in the Alpine region. The reanalysis IWV trends generally agree well with GNSS trends in Switzerland, but the spatial trend variability is not resolved by the reanalyses. Local measurements of IWV such as microwave radiometer, FTIR or GNSS measurements are therefore crucial to monitor changes in IWV, especially in mountainous regions such as Switzerland.

7 Conclusions

Our study presents trends of integrated water vapour (IWV) in Switzerland from a ground-based microwave radiometer, an FTIR spectrometer, GNSS stations and reanalysis data. We found that IWV generally increased by around 2 to 5 % per decade ~~in the last 24 years.~~ from 1995 to 2018. Using a straightforward trend approach that accounts for jumps due to instrumental changes, we found significant positive IWV trends for some GNSS stations in western and eastern Switzerland. Further, our data show that trend significance tends to be larger in summer and to increase with altitude (up to ~~1700 m~~ 1650 m a.s.l.).

Comparing IWV from the radiometer in Bern with GNSS and reanalyses showed a good agreement, with differences within 5 %. The FTIR spectrometer at the high altitude station Jungfraujoch revealed a constant clear-sky bias of 1 mm compared to GNSS data. Nevertheless, the IWV data and also the trends of both data sets at Jungfraujoch agree within their uncertainties when only coincident measurements are used. We further found that the ~~GNSS trends~~ IWV trends of the Swiss GNSS station network agree on average with the Swiss reanalysis trends ~~, but~~ (2.6 to 3.6 % per decade), but that the reanalyses are not able to capture regional variability, especially in the Alps. We conclude that GNSS data are reliable for the detection of climatic IWV trends. However, a few stations may require further quality control and harmonisation in the trend analysis.

Measurements in Bern reveal that the IWV trends follow observed temperature changes according to the Clausius-Clapeyron equation. Still, they do not scale to temperature as expected in some months, especially in winter, suggesting that other processes such as changes in dynamical patterns are responsible for IWV changes in winter. However, these winter trends are not significantly different from zero, which hinders us drawing robust conclusions about temperature related IWV changes in winter. Also, several colder winters in our study period might hide the long-term winter temperature increase in Switzerland. Nevertheless, ERA5 confirms the departure from Clausius-Clapeyron scaling in winter during our study period. This is not observed in MERRA-2 temperature data, which is spatially variable and resulting IWV changes disagree with the observed MERRA-2 IWV trends. This might be related to the poorly resolved topography in the larger MERRA-2 grids. The reanalysis grids probably miss regional variability in atmospheric stratification and convection, as it was also observed for zonal means by Wentz and Schabel (2000). Further, a bias in MERRA-2 tropospheric temperature was observed for several Alpine grids after 2017. This reflects the problematic of using reanalysis data for trend estimates due to changes in observing systems or assimilated data.

Another reason for observed inconsistencies between temperature and IWV changes might be changes in relative humidity (RH). Our temperature–IWV relation assumes that the relative humidity remains constant. However, we found positive RH trends in winter using lower tropospheric ERA5 data. Even though the RH trends are not significant, they might partly explain the disagreement between observed winter temperature and IWV changes. Wang et al. (2016) states that RH may not be constant because of limited moisture availability over land surfaces. Some studies found even a decrease of relative humidity with increasing temperature at midlatitudes (O'Gorman and Muller, 2010) or in the subtropics (Dessler et al., 2008). Further analyses with additional data sets would be required to provide more insights into possible RH trends in Switzerland.

It would be necessary to analyse temperature induced changes at more stations to draw robust conclusions about correlations between temperature and IWV changes. The problem of hidden long-term temperature trends in our study might be solved by using longer temperature time series, but longer IWV time series are sparse. Comparing regional IWV changes with tropospheric temperature changes from observations (e.g. radiosondes) rather than from reanalyses might be another approach to improve understanding of regional temperature–IWV relations. Nevertheless, it is generally difficult to attribute observed climate changes to unambiguous sources and feedbacks (Santer et al., 2007). Only complex attribution studies with multiple model runs can clarify this issue, as done for example by Santer et al. (2007) for IWV over oceans. However, global climate models lack feedbacks on the regional level (Sherwood et al., 2010), and studies based on regional observations are thus necessary.

~~Another reason for observed inconsistencies between temperature and IWV changes might be changes in relative humidity. Our temperature–IWV relation assumes that the relative humidity remains constant. However, this is not always the case, because of limited moisture availability over land surfaces (Wang et al., 2016). Some studies found even a decrease of relative humidity with increasing temperature at midlatitudes (O'Gorman and Muller, 2010) or in the subtropics (Dessler et al., 2008). Analysing local changes of relative humidity throughout the troposphere would be necessary to examine this assumption.~~

In summary, our results confirm the increase of water vapour with global warming on a regional scale, stressing the importance of the water vapour feedback. Further, the results emphasise the importance of regional IWV analyses, by showing that regional trend differences can be large, especially in mountainous areas. The spatial coverage of long-term IWV measurements from ground stations is sparse. We have shown that homogeneously reprocessed GNSS data have the potential to fill this gap and that they enable monitoring of regional water vapour trends in a changing climate. We further found that water vapour increase follows temperature changes as expected, ~~but the relationship is not everywhere clear~~except in winter. In a changing climate, it is therefore important to assess both, regional changes in temperature and water vapour, to understand and project possible changes in precipitation patterns and cloud formation on a regional scale.

Data availability. TROWARA and GNSS-derived IWV data are provided by the STARTWAVE database (http://www.iapmw.unibe.ch/research/projects/STARTWAVE/). The gap-filled TROWARA data used before 2008 are available on request. The Jungfraujoch FTIR data are publicly available from the Network for the Detection of Atmospheric Composition Change (NDACC) at ftp://ftp.cpc.ncep.noaa.gov/ndacc/station/jungfrau/hdf/ftir/. MERRA-2 data are available online through the NASA Goddard Earth Sciences Data Information Services Center (GES DISC) at https://disc.gsfc.nasa.gov/datasets?keywords=%22MERRA-2%22&page=1&source=Models%2FAnalyses%20MERRA-2. ERA5 data are available through the Copernicus Climate Change Service Climate Data Store (CDS) at https://cds.climate.copernicus.eu/cdsapp#!/home.

Author contributions. The study concept has been designed by LB and KH. LB analysed the data and prepared the manuscript. TvC provided the trend programme and GS provided the monthly resampling programme. EM was responsible for the FTIR data, EB for the GNSS data, and CM, NK and KH for the TROWARA data. All Co-Authors contributed to the manuscript preparation and the interpretation of the results.

Competing interests. The authors declare that they have no competing interests.

Acknowledgements. L. Bernet was funded by the Swiss National Science Foundation, grant number 200021-165516. We thank the technicians and engineers from the Institute of Applied Physics, University of Bern, who have kept TROWARA working since many years. The University of Liège's involvement has primarily been supported by the F.R.S. – FNRS (Fonds de la Recherche Scientifique) and the Belgian Federal Science Policy Office (BELSPO), both in Brussels, as well as by the GAW-CH programme of MeteoSwiss. The Fédération Wallonie Bruxelles contributed to supporting observational activities. E. Mahieu is a Research Associate with the F.R.S. – FNRS. We thank the International Foundation High Altitude Research Stations Jungfraujoch and Gornergrat (HFSJG, Bern) for supporting the facilities needed to perform the FTIR observations and the many colleagues who contributed to FTIR data acquisition at that site. The 10.7cm solar radio flux data were provided as a service by the National Research Council of Canada and distributed in partnership with Natural Resources Canada. E. Brockmann from swisstopo provided the GNSS-derived ZTD data (operationally and reprocessed) for all Swiss stations.

References

AGNES swisstopo: Automated GNSS Network for Switzerland (AGNES), http://pnac.swisstopo.admin.ch/pages/en/agnes.html, last access: 14 June 2020.

Alshawaf, F., Balidakis, K., Dick, G., Heise, S., and Wickert, J.: Estimating trends in atmospheric water vapor and temperature time series over Germany, Atmos. Meas. Tech., 10, 3117–3132, https://doi.org/10.5194/amt-10-3117-2017, 2017.

Armour, K. C., Bitz, C. M., and Roe, G. H.: Time-Varying Climate Sensitivity from Regional Feedbacks, J. Clim., 26, 4518–4534, https://doi.org/10.1175/JCLI-D-12-00544.1, 2013.

Begert, M. and Frei, C.: Long-term area-mean temperature series for Switzerland—Combining homogenized station data and high resolution grid data, Int. J. Climatol., 38, 2792–2807, https://doi.org/10.1002/joc.5460, 2018.

Bengtsson, L., Hagemann, S., and Hodges, K. I.: Can climate trends be calculated from reanalysis data?, J. Geophys. Res. D Atmos., 109, D11 111, https://doi.org/10.1029/2004JD004536, 2004.

Bernet, L., von Clarmann, T., ~~Godin-beekmann~~Godin-Beekmann, S., Ancellet, G., ~~and~~ Maillard Barras, E., Stübi, R., Steinbrecht, W., Kämpfer, N., and Hocke, K.: Ground-based ozone profiles over central Europe: incorporating anomalous observations into the analysis of stratospheric ozone trends, Atmos. Chem. Phys., 19, 4289–4309, https://doi.org/10.5194/acp-19-4289-2019, https://www.atmos-chem-phys.net/19/4289/2019/, 2019.

Bevis, M., Businger, S., Herring, T. A., Rocken, C., Anthes, R. A., and Ware, R. H.: GPS meteorology: Remote sensing of atmospheric water vapor using the global positioning system, J. Geophys. Res., 97, 15 787–15 801, https://doi.org/10.1029/92JD01517, 1992.

Bock, O. and Parracho, A. C.: Consistency and representativeness of integrated water vapour from ground-based GPS observations and ERA-Interim reanalysis, Atmos. Chem. Phys., 19, 9453–9468, https://doi.org/10.5194/acp-2019-28, 2019.

Bock, O., Keil, C., Richard, E., Flamant, C., and Bouin, M. N.: Validation for precipitable water from ECMWF model analyses with GPS and radiosonde data during the MAP SOP, Q. J. R. Meteorol. Soc., 131, 3013–3036, https://doi.org/10.1256/qj.05.27, 2005.

Brockmann, E.: Positionierungsdienste und Geodaten des Schweizerischen Bundesamtes für Landestopographie, in: Tagungsband - POSNAV 2001, DGON-Symposium Positionierung und Navig. 6. bis 8. März 2001, Dresden, DGON, Bonn, 2001.

Brockmann, E.: Reprocessed GNSS tropospheric products at swisstopo, GNSS4SWEC workshop, Thessaloniki, May 11-14 2015, 2015.

Brockmann, E., Grünig, S., Hug, R., Schneider, D., Wiget, A., and Wild, U.: National Report of Switzerland Introduction and first applications of a Real-Time Precise Positioning Service using the Swiss Permanent Network, in: ~~Subcomm. Eur. Ref. Fram.~~ Subcommission for the European Reference Frame (EUREF). EUREF ~~Publ.~~ Publication No. 10, edited by Torres, J. and Hornik, H., pp. 272–276, Mitteilungen des Bundesamtes für Kartographie und Geodäsie, Vol. 23, Frankfurt am Main 2002, http://www.euref.eu/symposia/book2001/nr_28.PDF, 2001a.

Brockmann, E., Guerova, G., and Troller, M.: Swiss Activities in Combining GPS with Meteorology, in: Subcommission for the European Reference Frame (EUREF). EUREF Publication No. 10, edited by Torres, J. and Hornik, H., pp. 95–99, Mitteilungen des Bundesamtes für Kartographie und Geodäsie, Vol. 23, Frankfurt am Main 2002, http://www.euref.eu/symposia/book2001/2_6.pdf, 2001b.

Brockmann, E., Andrey, D., Ineichen, D., Kislig, L., Liechti, J., Lutz, S., Misslin, C., Schaer, S., and Wild, U.: Automated GNSS Network Switzerland (AGNES), International Foundation HFSJG, Activity Report 2016, https://www.hfsjg.ch/wordpress/reports/2016/137_Swisstopo_Brockmann.pdf, 2016.

Brockmann, E., Andrey, D., Ineichen, D., Lutz, S., Wild, U., Vapor, I. W., and Delay, Z. P.: Automated GNSS Network Switzerland (AGNES), International Foundation HFSJG, Activity Report 2019, 2019.

Chen, B. and Liu, Z.: Global water vapor variability and trend from the latest 36 year (1979 to 2014) data of ECMWF and NCEP reanalyses, radiosonde, GPS, and microwave satellite, J. Geophys. Res., 121, 11 442–11 462, https://doi.org/10.1002/2016JD024917, 2016.

Copernicus CDS: ERA5 monthly averaged data on single levels from 1979 to present, ~~,~~https://cds.climate.copernicus.eu/cdsapp#!/dataset/reanalysis-era5-single-levels-monthly-means?tab=overview, last access: 30 April 2019, a.

Copernicus CDS: ERA5 monthly averaged data on pressure levels from 1979 to present, ~~,~~https://cds.climate.copernicus.eu/cdsapp#!/dataset/reanalysis-era5-pressure-levels-monthly-means?tab=overview, last access: 8 October 2019, b.

Copernicus Climate Change Service (C3S): ERA5: Fifth generation of ECMWF atmospheric reanalyses of the global climate, https://cds.climate.copernicus.eu/cdsapp#!/home, last access: 14 June 2020, 2017.

Davis, J. L., Herrinch, T. A., Shapiro, I. I., Rogers, A. E. E., and Elgered, G.: Geodesy by radio interferometry: Effects of atmospheric modeling errors on estimates of baseline length, Radio Sci., 20, 1593–1607, 1985.

Dee, D. P., Uppala, S. M., Simmons, A. J., Berrisford, P., Poli, P., Kobayashi, S., Andrae, U., Balmaseda, M. A., Balsamo, G., Bauer, P., Bechtold, P., Beljaars, A. C., van de Berg, L., Bidlot, J., Bormann, N., Delsol, C., Dragani, R., Fuentes, M., Geer, A. J., Haimberger, L., Healy, S. B., Hersbach, H., Hólm, E. V., Isaksen, L., Kållberg, P., Köhler, M., Matricardi, M., Mcnally, A. P., Monge-Sanz, B. M., Morcrette, J. J., Park, B. K., Peubey, C., de Rosnay, P., Tavolato, C., Thépaut, J. N., and Vitart, F.: The ERA-Interim reanalysis: Configuration and performance of the data assimilation system, Q. J. R. Meteorol. Soc., 137, 553–597, https://doi.org/10.1002/qj.828, 2011.

Dessler, A. E., Yang, P., Lee, J., Solbrig, J., Zhang, Z., and Minschwaner, K.: An analysis of the dependence of clear-sky top-of-atmosphere outgoing longwave radiation on atmospheric temperature and water vapor, J. Geophys. Res., 113, D17 102, https://doi.org/10.1029/2008JD010137, 2008.

Eckert, E., von Clarmann, T., Kiefer, M., Stiller, G. P., Lossow, S., Glatthor, N., Degenstein, D. A., Froidevaux, L., Godin-Beekmann, S., Leblanc, T., McDermid, S., Pastel, M., Steinbrecht, W., Swart, D. P. J., Walker, K. A., and Bernath, P. F.: Drift-corrected trends and periodic variations in MIPAS IMK/IAA ozone measurements, Atmos. Chem. Phys., 14, 2571–2589, https://doi.org/10.5194/acp-14-2571-2014, 2014.

Elgered, G., Davis, J. L., Herring, T. A., and Shapiro, I. I.: Geodesy by Radio Interferometry: Water Vapor Radiometry for Estimation of the Wet Delay, J. Geophys. Res., 96, 6541–6555, 1991.

~~Fujita, M. and Sato, T.: Observed behaviours of precipitable water vapour and precipitation intensity in response to upper air profiles estimated from surface air temperature, Sci. Rep., 7, 5–10, , 2017.~~

Gelaro, R., McCarty, W., Suárez, M. J., Todling, R., Molod, A., Takacs, L., Randles, C. A., Darmenov, A., Bosilovich, M. G., Reichle, R., Wargan, K., Coy, L., Cullather, R., Draper, C., Akella, S., Buchard, V., Conaty, A., da Silva, A. M., Gu, W., Kim, G. K., Koster, R., Lucchesi, R., Merkova, D., Nielsen, J. E., Partyka, G., Pawson, S., Putman, W., Rienecker, M., Schubert, S. D., Sienkiewicz, M., and Zhao, B.: The Modern-Era Retrospective Analysis for Research and Applications, version 2 (MERRA-2), J. Clim., 30, 5419–5454, https://doi.org/10.1175/JCLI-D-16-0758.1, 2017.

Gerber, C.: Combining measurements from the microwave radiometers TROWARA and GROMOS for improved trend analysis of the integrated water vapour, Bachelor thesis, University of Bern, 2009.

Global Modeling and Assimilation Office (GMAO): MERRA-2 instM~~_~~_2d~~_int_~~_int_Nx: 2d, Monthly mean, Instantaneous, Single-Level, Assimilation, Vertically Integrated Diagnostics V5.12.4, Goddard Earth Sciences Data and Information Services Center (GES DISC), Greenbelt, MD, USA, https://doi.org/10.5067/KVTU1A8BWFSJ, 2015a.

Global Modeling and Assimilation Office (GMAO): MERRA-2 instM~~_~~_3d~~_asm_~~_asm_Np: 3d, Monthly mean, Instantaneous, Pressure-Level, Assimilation, Assimilated Meteorological Fields V5.12.4, Goddard Earth Sciences Data and Information Services Center (GES DISC), Greenbelt, MD, USA, https://doi.org/10.5067/2E096JV59PK7, 2015b.

Gradinarsky, L. P., Johansson, J. M., Bouma, H. R., Scherneck, H. G., and Elgered, G.: Climate monitoring using GPS, Phys. Chem. Earth, 27, 335–340, https://doi.org/10.1016/S1474-7065(02)00009-8, 2002.

Gubler, S., Gruber, S., and Purves, R. S.: Uncertainties of parameterized surface downward clear-sky shortwave and all-sky longwave radiation, Atmos. Chem. Phys., 12, 5077–5098, https://doi.org/10.5194/acp-12-5077-2012, 2012.

Guerova, G., Brockmann, E., Quiby, J., Schubiger, F., and Mätzler, C.: Validation of NWP Mesoscale Models with Swiss GPS Network AGNES, J. Appl. Meteorol., 42, 141–150, https://doi.org/10.1175/1520-0450(2003)042<0141:vonmmw>2.0.co;2, 2003.

Haefele, P., Martin, L., Becker, M., Brockmann, E., Morland, J., Nyeki, S., Mätzler, C., and Kirchner, M.: Impact of radiometrie water vapor measurements on troposphere and height estimates by GPS, in: ~~Proc.~~ Proceedings of the 17th ~~Int. Tech. Meet. Satell. Div. Inst. Navig.~~ International Technical Meeting of the Satellite Division of the Institute of Navigation, ION GNSS 2004, pp. 2289–2302, Long Beach, CA, 2004.

Hagemann, S., Bengtsson, L., and Gendt, G.: On the determination of atmospheric water vapour from GPS measurements, Tech. Rep. 340, Max Planck Institute for Meteorology, Hamburg, Germany, 2002.

Hartmann, D., Tank, A. K., Rusticucci, M., Alexander, L., Brönnimann, S., Charabi, Y., Dentener, F., Dlugokencky, E., Easterling, D., Kaplan, A., Soden, B., Thorne, P., Wild, M., and P.M. Zhai: Observations: Atmosphere and Surface, in: Climate Change 2013: The Physical Science Basis. Contribution of Working Group I to the Fifth Assessment Report of the Intergovernmental Panel on Climate Change, edited by Stocker, T., Qin, D., Plattner, G.-K., Tignor, M., Allen, S., Boschung, J., Nauels, A., Xia, Y., Bex, V., and Midgley, P., chap. 2, pp. 159–254, Cambridge University Press, Cambridge, https://doi.org/10.1017/CBO9781107415324.008, 2013.

Heise, S., Dick, G., Gendt, G., Schmidt, T., and Wickert, J.: Integrated water vapor from IGS ground-based GPS observations: Initial results from a global 5-min data set, Ann. Geophys., 27, 2851–2859, https://doi.org/10.5194/angeo-27-2851-2009, 2009.

Held, I. M. and Soden, B. J.: Water Vapor Feedback and Global Warming, Annu. Rev. Energy Environ., 25, 441–475, 2000.

Hersbach, H., De Rosnay, P., Bell, B., Schepers, D., Simmons, A., Soci, C., Abdalla, S., Balmaseda, A., Balsamo, G., Bechtold, P., Berrisford, P., Bidlot, J., De Boisséson, E., Bonavita, M., Browne, P., Buizza, R., Dahlgren, P., Dee, D., Dragani, R., Diamantakis, M., Flemming, J., Forbes, R., Geer, A., Haiden, T., Hólm, E., Haimberger, L., Hogan, R., Horányi, A., Janisková, M., Laloyaux, P., Lopez, P., Muñoz-Sabater, J., Peubey, C., Radu, R., Richardson, D., Thépaut, J.-N., Vitart, F., Yang, X., Zsótér, E., and Zuo, H.: Operational global reanalysis: progress, future directions and synergies with NWP including updates on the ERA5 production status, in: ERA Rep. Ser. No. 27, European Centre for Medium Range Weather Forecasts (ECMWF), Reading, England, https://doi.org/10.21957/tkic6g3wm, 2018.

Hicks-Jalali, S., Sica, R. J., Haefele, A., Martucci, G., Maillard Barras, E., and Voirin, J.: A Raman Lidar Tropospheric Water Vapour Climatology and Height-Resolved Trend Analysis over Payerne Switzerland, Atmos. Chem. Phys. Discuss., pp. 1–29, https://doi.org/10.5194/acp-2019-1089, 2020.

Ho, S. P., Peng, L., Mears, C., and Anthes, R. A.: Comparison of global observations and trends of total precipitable water derived from microwave radiometers and COSMIC radio occultation from 2006 to 2013, Atmos. Chem. Phys., 18, 259–274, https://doi.org/10.5194/acp-18-259-2018, 2018.

Hocke, K., Kämpfer, N., Gerber, C., and Mätzler, C.: A complete long-term series of integrated water vapour from ground-based microwave radiometers, Int. J. Remote Sens., 32, 751–765, https://doi.org/10.1080/01431161.2010.517792, 2011.

Hocke, K., Navas Guzmán, F., Cossu, F., and Mätzler, C.: Cloud Fraction of Liquid Water Clouds above Switzerland over the Last 12 Years, Climate, 4, 48, https://doi.org/10.3390/cli4040048, http://www.mdpi.com/2225-1154/4/4/48, 2016.

Hocke, K., Navas-Guzmán, F., Moreira, L., Bernet, L., and Mätzler, C.: Oscillations in atmospheric water above Switzerland, Atmos. Chem. Phys., 17, 12 121–12 131, https://doi.org/10.5194/acp-17-12121-2017, 2017.

Hocke, K., Bernet, L., Hagen, J., Murk, A., Renker, M., and Mätzler, C.: Diurnal cycle of short-term fluctuations of integrated water vapour above Switzerland, Atmos. Chem. Phys., 19, 12 083–12 090, https://doi.org/10.5194/acp-19-12083-2019, https://www.atmos-chem-phys.net/19/12083/2019/, 2019.

Ingold, T., Peter, R., and Kämpfer, N.: Weighted mean tropospheric temperature and transmittance determination at millimeter-wave frequencies for ground-based applications, Radio Sci., 33, 905–918, https://doi.org/10.1002/zaac.200400263, 1998.

Ingold, T., Schmid, B., Mätzler, C., Demoulin, P., and Kämpfer, N.: Modeled and empirical approaches for retrieving columnar water vapor from solar tranmittance measurements in the 0.72, 0.82, and 0.94 μm absorption bands, J. Geophys. Res., 105, 24 327–24 343, 2000.

IPCC: Summary for Policymakers, in: Climate Change 2013: The Physical Science Basis. Contribution of Working Group I to the Fifth Assessment Report of the Intergovernmental Panel on Climate Change, edited by Stocker, T., Qin, D., Plattner, G.-K., Tignor, M., Allen, S., Boschung, J., Nauels, A., Xia, Y., Bex, V., and Midgley, P., Cambridge University Press, Cambridge, United Kingdom and New York, NY, USA, https://doi.org/10.1017/CBO9781107415324.004, 2013.

John, V. O., Holl, G., Allan, R. P., Buehler, S. A., Parker, D. E., and Soden, B. J.: Clear-sky biases in satellite infrared estimates of upper tropospheric humidity and its trends, J. Geophys. Res. Atmos., 116, D14 108, https://doi.org/10.1029/2010JD015355, 2011.

Kämpfer, N.: Introduction, in: Monitoring Atmospheric Water Vapour. ~~Ground-based~~ Ground-Based Remote Sensing and In-situ Methods, edited by Kämpfer, N., chap. 1, pp. 1–7, Springer New York, New York, NY, https://doi.org/10.1007/978-1-4614-3909-7_1, 2013.

Mätzler, C. and Morland, J.: Refined physical retrieval of integrated water vapor and cloud liquid for microwave radiometer data, IEEE Trans. Geosci. Remote Sens., 47, 1585–1594, https://doi.org/10.1109/TGRS.2008.2006984, 2009.

MeteoSwiss (Federal Institute for Meteorology and Climatology): Temperature and precipitation trends, https://www.meteoswiss.admin.ch/home/climate/climate-change-in-switzerland/temperature-and-precipitation-trends.html?filters=ths200m0_swiss_djf_1864-smoother, 2019.

Mieruch, S., Noël, S., Bovensmann, H., and Burrows, J. P.: Analysis of global water vapour trends from satellite measurements in the visible spectral range, Atmos. Chem. Phys., 8, 491–504, https://doi.org/10.5194/acp-8-491-2008, 2008.

Möller, F.: On the influence of changes in the CO 2 concentration in air on the radiation balance of the Earth's surface and on the climate , J. Geophys. Res., 68, 3877–3886, https://doi.org/10.1029/jz068i013p03877, 1963.

Morland, J.: TROWARA - Tropospheric Water Vapour Radiometer. Radiometer review and new calibration model ., Tech. rep., University of Bern, Bern, Switzerland, 2002.

Morland, J., Deuber, B., Feist, D. G., Martin, L., Nyeki, S., Kämpfer, N., Mätzler, C., Jeannet, P., and Vuilleumier, L.: The STARTWAVE atmospheric water database, Atmos. Chem. Phys., 6, 2039–2056, www.atmos-chem-phys.net/6/2039/2006/, 2006.

Morland, J., Coen, C. M., Hocke, K., Jeannet, P., and Mätzler, C.: Tropospheric water vapour above Switzerland over the last 12 years, Atmos. Chem. Phys., 9, 5975–5988, https://doi.org/10.5194/acp-9-5975-2009, 2009.

National Research Council of Canada: Latest Solar Radio Flux Report from DRAO, Penticton, https://www.spaceweather.gc.ca/solarflux/sx-5-mavg-en.php, ~~2019.~~ last access: 14 June 2020.

NCCS: CH2018 – Climate Scenarios for Switzerland, p. 271, Technical Report, National Centre for Climate Services, Zurich, 2018.

Nilsson, T. and Elgered, G.: Long-term trends in the atmospheric water vapor content estimated from ground-based GPS data, J. Geophys. Res. Atmos., 113, https://doi.org/10.1029/2008JD010110, 2008.

Ning, T., Wang, J., Elgered, G., Dick, G., Wickert, J., Bradke, M., Sommer, M., Querel, R., and Smale, D.: The uncertainty of the atmospheric integrated water vapour estimated from GNSS observations, Atmos. Meas. Tech., 9, 79–92, https://doi.org/10.5194/amt-9-79-2016, 2016a.

Ning, T., Wickert, J., Deng, Z., Heise, S., Dick, G., Vey, S., and Schöne, T.: Homogenized time series of the atmospheric water vapor content obtained from the GNSS reprocessed data, J. Clim., 29, 2443–2456, https://doi.org/10.1175/JCLI-D-15-0158.1, ~~2016.~~ 2016b.

Nyeki, S., Vuilleumier, L., Morland, J., Bokoye, A., Viatte, P., Mätzler, C., and Kämpfer, N.: A 10-year integrated atmospheric water vapor record using precision filter radiometers at two high-alpine sites, Geophys. Res. Lett., 32, L23 803, https://doi.org/10.1029/2005GL024079, 2005.

Nyeki, S., Wacker, S., Aebi, C., Gröbner, J., Martucci, G., and Vuilleumier, L.: Trends in surface radiation and cloud radiative effect at four Swiss sites for the 1996–2015 period, Atmos. Chem. Phys., 19, 13 227–13 241, https://doi.org/10.5194/acp-19-13227-2019, 2019.

O'Gorman, P. A. and Muller, C. J.: How closely do changes in surface and column water vapor follow Clausius-Clapeyron scaling in climate change simulations?, Environ. Res. Lett., 5, https://doi.org/10.1088/1748-9326/5/2/025207, 2010.

Pacione, R., Araszkiewicz, A., Brockmann, E., and Dousa, J.: EPN-Repro2: A reference GNSS tropospheric data set over Europe, Atmos. Meas. Tech., 10, 1689–1705, https://doi.org/10.5194/amt-10-1689-2017, 2017.

Parracho, A. C., Bock, O., and Bastin, S.: Global IWV trends and variability in atmospheric reanalyses and GPS observations, Atmos. Chem. Phys., 18, 16 213–16 237, https://doi.org/10.5194/acp-18-16213-2018, 2018.

Pepin, N., Bradley, R. S., Diaz, H. F., Baraer, M., Caceres, E. B., Forsythe, N., Fowler, H., Greenwood, G., Hashmi, M. Z., Liu, X. D., Miller, J. R., Ning, L., Ohmura, A., Palazzi, E., Rangwala, I., Schöner, W., Severskiy, I., Shahgedanova, M., Wang, M. B., Williamson, S. N., and Yang, D. Q.: Elevation-dependent warming in mountain regions of the world, Nat. Clim. Chang., 5, 424–430, https://doi.org/10.1038/nclimate2563, 2015.

Peter, R. and Kämpfer, N.: Radiometric Determination of Water Vapor and Liquid Water and Its Validation With Other Techniques, J. Geophys. Res., 97, 18 173–18 183, 1992.

Ross, R. J. and Elliot, W. P.: Radiosonde-based Northern Hemisphere tropospheric water vapor trends, J. Clim., 14, 1602–1612, https://doi.org/10.1175/1520-0442(2001)014<1602:RBNHTW>2.0.CO;2, 2001.

Saastamoinen, J.: Atmospheric Correction for the Troposphere and Stratosphere in Radio Ranging Satellites, in: ~~Use Artif. Satell. Geod.~~The Use of Artificial Satellites for Geodesy, edited by S. W. Henriksen et al., vol. 15, pp. 247–251, Geophys. Monogr. Ser., Washington, D.C., https://doi.org/10.1029/GM015p0247, 1972.

Santer, B. D., Mears, C., Wentz, F. J., Taylor, K. E., Gleckler, P. J., Wigley, T. M. L., Barnett, T. P., Boyle, J. S., Bruggemann, W., Gillett, N. P., Klein, S. A., Meehl, G. A., Nozawa, T., Pierce, D. W., Stott, P. A., Washington, W. M., and Wehner, M. F.: Identification of human-induced changes in atmospheric moisture content, Proc. Natl. Acad. Sci., 104, 15 248–15 253, https://doi.org/10.1073/pnas.0702872104, 2007.

Schneider, D., Brockmann, E., Marti, U., Schlatter, A., and Wild, U.: National Report of Switzerland Introduction of a Precise Swiss Positioning Service "swipos" and Progress in the Swiss National Height Network " LHN95 ", in: ~~Rep. Symp. IAG Subcomm. Eur. held~~ Report on the Symposium of the IAG Subcommission for Europe (EUREF) held in Tromsø, 22 - 24 June 2000, edited by Torres, J., pp. 315–322, 2000.

Schneider, M., Romero, P. M., Hase, F., Blumenstock, T., Cuevas, E., and Ramos, R.: Continuous quality assessment of atmospheric water vapour measurement techniques: FTIR, Cimel, MFRSR, GPS, and Vaisala RS92, Atmos. Meas. Tech., 3, 323–338, https://doi.org/10.5194/amt-3-323-2010, 2010.

Schneider, M., Barthlott, S., Hase, F., González, Y., Yoshimura, K., García, O. E., Sepúlveda, E., Gomez-Pelaez, A., Gisi, M., Kohlhepp, R., Dohe, S., Blumenstock, T., Wiegele, A., Christner, E., Strong, K., Weaver, D., Palm, M., Deutscher, N. M., Warneke, T., Notholt, J., Lejeune, B., Demoulin, P., Jones, N., Griffith, D. W., Smale, D., and Robinson, J.: Ground-based remote sensing of tropospheric water vapour isotopologues within the project MUSICA, Atmos. Meas. Tech., 5, 3007–3027, https://doi.org/10.5194/amt-5-3007-2012, 2012.

Sherwood, S. C., Roca, R., Weckwerth, T. M., and Andronova, N. G.: Tropospheric water vapor, convection, and climate, Rev. Geophys., 48, RG2001, https://doi.org/10.1029/2009RG000301, 2010.

Stocker, T. F., Clarke, G., Treut, H. L., Lindzen, R., Meleshko, V., Mugara, R., Palmer, T., Pierrehumbert, R., Sellers, P., Trenberth, K., and Willebrand, J.: Physical Climate Processes and Feedbacks, in: Climate Change 2001: The Scientific Basis. Contribution of Working Group I to the Third Assessment Report of the Intergovernmental Panel on Climate Change, edited by Houghton, J., Ding, Y., Griggs, D., Noguer, M., van der Linden, P., Dai, X., Maskell, K., and Johnson, C., chap. 7, pp. 417–470, Cambridge University Press, Cambridge, United Kingdom and New York, NY, USA,, 2001.

Sussmann, R., Borsdorff, T., Rettinger, M., Camy-Peyret, C., Demoulin, P., Duchatelet, P., Mahieu, E., and Servais, C.: Technical Note: Harmonized retrieval of column-integrated atmospheric water vapor from the FTIR network – First examples for long-term records and station trends, Atmos. Chem. Phys., 9, 8987–8999, https://doi.org/10.5194/acp-9-8987-2009, 2009.

~~Swisstopo: Automated GNSS Network for Switzerland (AGNES), , 2019.~~

Thayer, G. D.: An improved equation for the radio refractive index of air, Radio Sci., 9, 803–807, https://doi.org/10.1029/RS009i010p00803, 1974.

Trenberth, K. E., Fasullo, J., and Smith, L.: Trends and variability in column-integrated atmospheric water vapor, Clim. Dyn., 24, 741–758, https://doi.org/10.1007/s00382-005-0017-4, 2005.

Urban, J.: Satellite Sensors Measuring Atmospheric Water Vapour, in: Monitoring Atmospheric Water Vapour. ~~Ground-based~~ Ground-Based Remote Sensing and In-situ Methods, edited by Kämpfer, N., chap. 9, pp. 175–214, Springer New York, New York, NY, https://doi.org/10.1007/978-1-4614-3909-7, 2013.

Vey, S., Dietrich, R., Fritsche, M., Rülke, A., Steigenberger, P., and Rothacher, M.: On the homogeneity and interpretation of precipitable water time series derived from global GPS observations, J. Geophys. Res. Atmos., 114, D10 101, https://doi.org/10.1029/2008JD010415, 2009.

von Clarmann, T., Grabowski, U., and Kiefer, M.: On the role of non-random errors in inverse problems in radiative transfer and other applications, J. Quant. Spectrosc. Radiat. Transf., 71, 39–46, https://doi.org/10.1016/S0022-4073(01)00010-3, 2001.

von Clarmann, T., Stiller, G. P., Grabowski, U., Eckert, E., and Orphal, J.: Technical note: Trend estimation from irregularly sampled, correlated data, Atmos. Chem. Phys., 10, 6737–6747, https://doi.org/10.5194/acp-10-6737-2010, 2010.

Wagner, T., Beirle, S., Grzegorski, M., and Platt, U.: Global trends (1996-2003) of total column precipitable water observed by Global Ozone Monitoring Experiment (GOME) on ERS-2 and their relation to near-surface temperature, J. Geophys. Res. Atmos., 111, D12 102, https://doi.org/10.1029/2005JD006523, 2006.

Wang, J., Dai, A., and Mears, C.: Global water vapor trend from 1988 to 2011 and its diurnal asymmetry based on GPS, radiosonde, and microwave satellite measurements, J. Clim., 29, 5205–5222, https://doi.org/10.1175/JCLI-D-15-0485.1, 2016.

Wehrli, C.: Calibrations of filter radiometers for determination of atmospheric optical depth, Metrologia, 37, 419–422, https://doi.org/10.1088/0026-1394/37/5/16, 2000.

Wentz, F. J. and Schabel, M.: Precise climate monitoring using complementary satellite data sets, Nature, 403, 414–416, https://doi.org/10.1038/35000184, 2000.

Wentz, F. J., Ricciardulli, L., Hilburn, K., and Mears, C.: How much more rain will global warming bring?, Science~~(80-.).~~, 317, 233–235, https://doi.org/10.1126/science.1140746, 2007.

Wilhelm, S., Stober, G., and Brown, P.: Climatologies and long-term changes in mesospheric wind and wave measurements based on radar observations at high and mid latitudes, Ann. Geophys., 37, 851–875, https://doi.org/10.5194/angeo-37-851-2019, 2019.

Zander, R., Mahieu, E., Demoulin, P., Duchatelet, P., Roland, G., Servais, C., Mazière, M. D., Reimann, S., and Rinsland, C. P.: Our changing atmosphere: Evidence based on long-term infrared solar observations at the Jungfraujoch since 1950, Sci. Total Environ., 391, 184–195, https://doi.org/10.1016/j.scitotenv.2007.10.018, 2008.

Zhang, Y., Xu, J., Yang, N., and Lan, P.: Variability and Trends in Global Precipitable Water Vapor Retrieved from COSMIC Radio Occultation and Radiosonde Observations, Atmosphere~~(Basel).~~, 9, https://doi.org/10.3390/atmos9050174, 2018.

GNSS stations in Switzerland

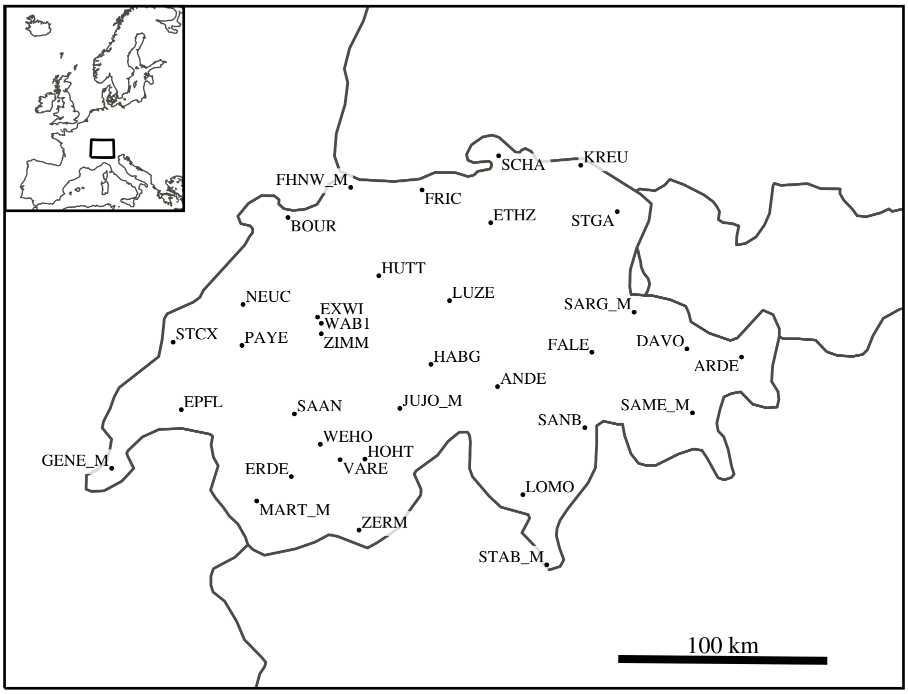

Figure 1. Map of Swiss Global Navigation Satellite System (GNSS) stations used in this study.

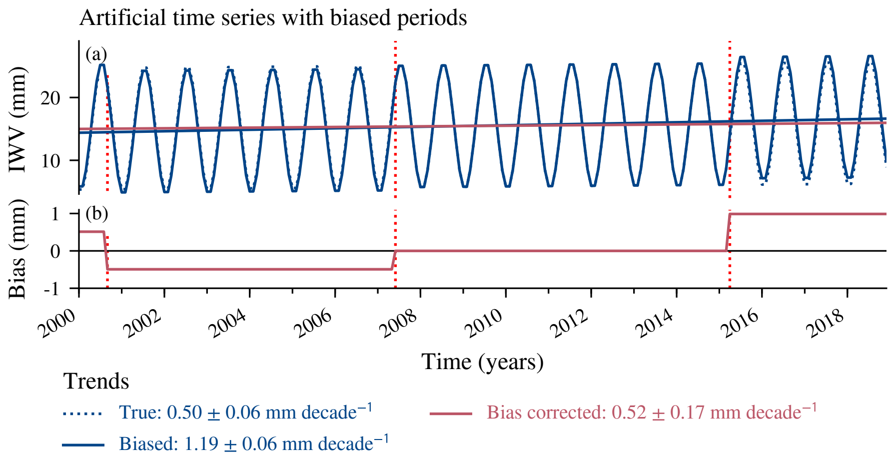

Figure 2. Artificial time series **(a)** and added biases **(b)**. The linear trends for the true (unbiased) data, the biased data and the bias corrected data are given.

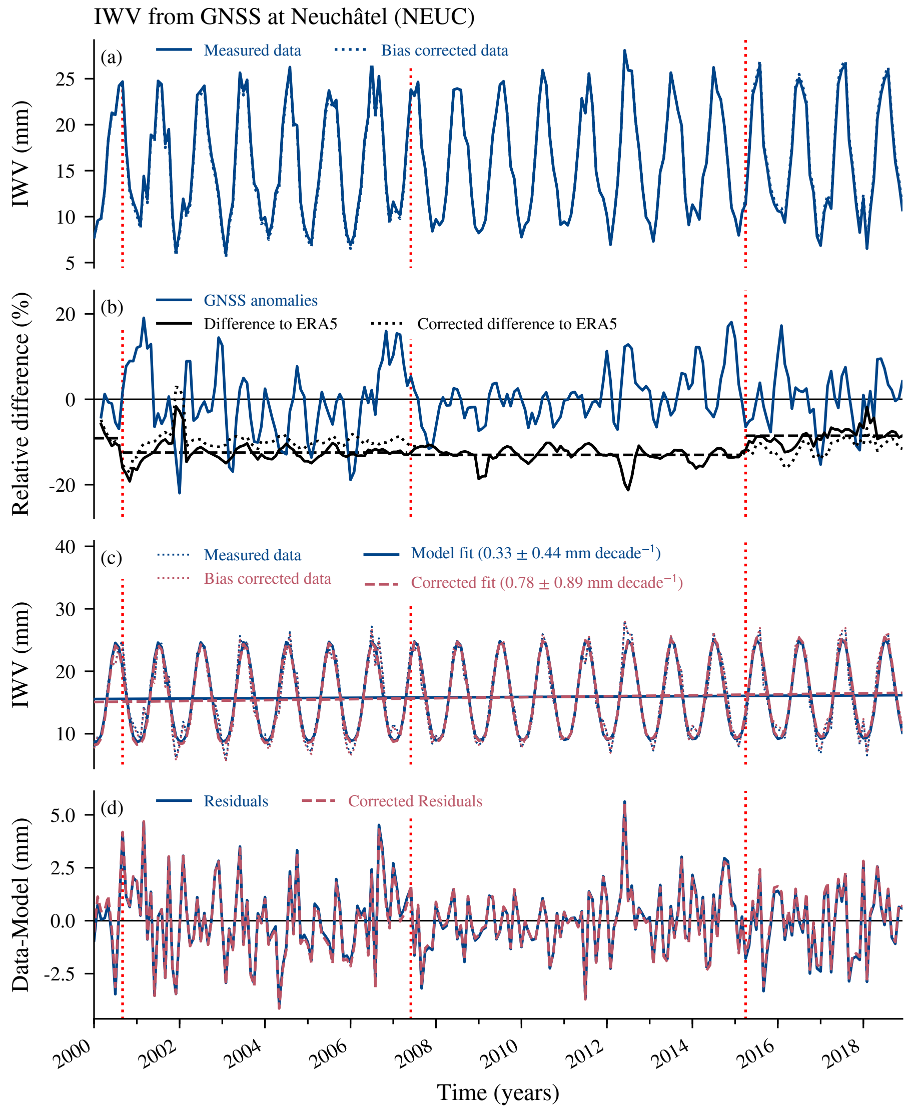

Figure 3. **(a)** Monthly means of integrated water vapour (IWV) from the GNSS station at Neuchâtel (NEUC), Switzerland. Changes in antenna ~~and receiver~~ types are indicated in all panels by vertical red dotted lines. **(b)** Anomalies from the climatology ((data−climatology)/climatology) of the GNSS data at Neuchâtel and relative difference to ERA5 data at the same location ((ERA5−GNSS)/GNSS), both smoothed with a three-months moving mean window. The horizontal black dashed lines show the averaged difference to ERA5 for each antenna change. The relative difference of the bias corrected GNSS data to ERA5 is also shown (dotted line). **(c)** Regression model fit and **(d)** residuals of the model ~~with and~~ without bias correction and with correction by considering data jumps in the trend model. The given trend uncertainties correspond to 2 standard deviations (σ).

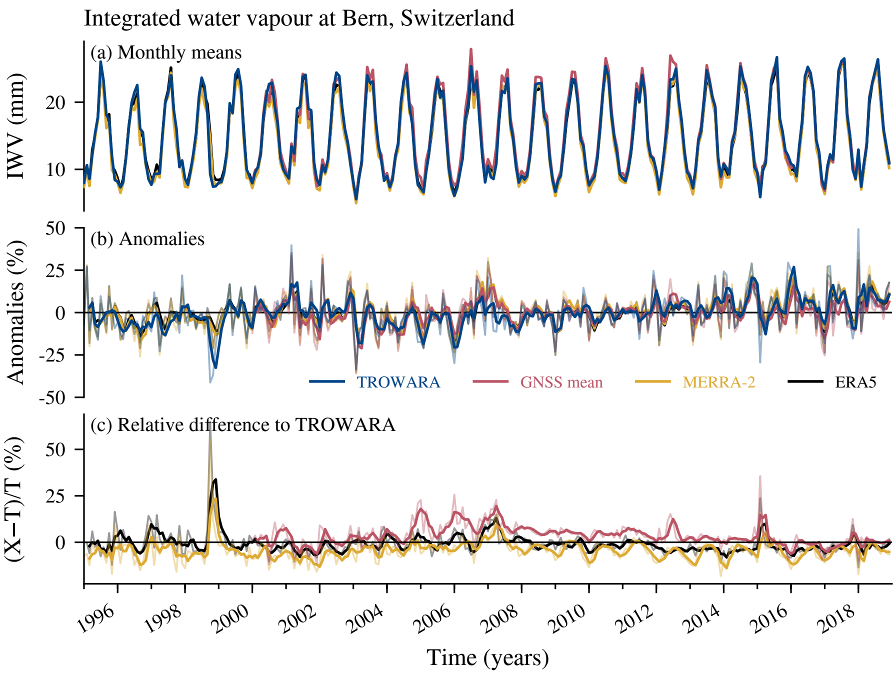

Figure 4. **(a)** Monthly means of IWV from the microwave radiometer TROWARA in Bern (Switzerland), from GNSS stations close to Bern, and from reanalysis grids (MERRA-2 and ERA5) at Bern. **(b)** Anomalies from the climatology ((data−climatology)/climatology) for each of the mentioned data sets. **(c)** Relative differences of the mentioned dataset X to TROWARA (T) data ($(\mathrm{X}-\mathrm{T})/\mathrm{T}$). The bold lines in **(b)** and **(c)** show the data smoothed with a moving mean window of three months, the thin pale lines show the unsmoothed monthly data.

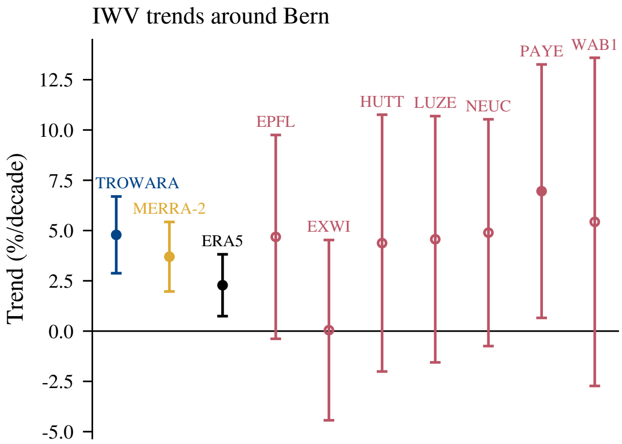

Figure 5. IWV trends for TROWARA ~~(TRO)~~ in Bern, reanalysis ~~grids~~ (MERRA-2 and ERA5) grid points at Bern and GNSS stations close to Bern. The error bars show 2 σ uncertainties. Filled dots represent trends that are significantly different from zero at 95% confidence interval.

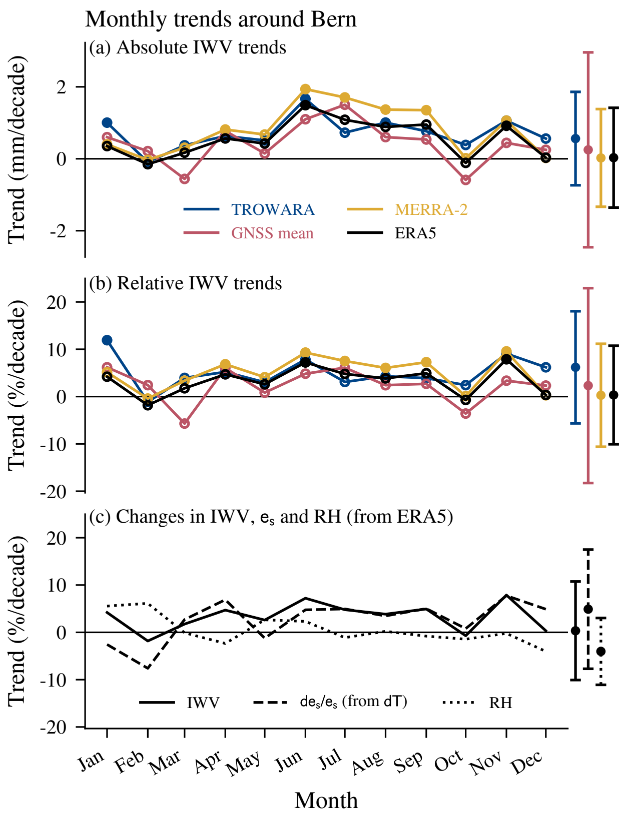

Figure 6. Trends of IWV for different months for TROWARA in Bern, GNSS stations close to Bern (arithmetic mean), and reanalysis grids (MERRA-2 and ERA5) at Bern. ~~Panel **(a)** shows~~ Uncertainty bars show the maximum range of $2\,\sigma$ uncertainties of each dataset. Filled dots represent trends that are significantly different from zero at 95% confidence interval. Monthly IWV trends are given in panel **(a)** as absolute trends in mm per decade ~~. Panel~~ and in panel **(b)** ~~shows IWV~~ as relative trends in percent per decade. Panel **(c)** presents again the monthly IWV trends from ERA5, and in addition the relative humidity (RH) trends and the theoretical change in saturation vapour pressure e_s due to the observed temperature change from ~~reanalysis~~ ERA5 data (both averaged below 500 hPa). ~~Filled dots represent trends that are significantly different from zero at 95% confidence interval.~~

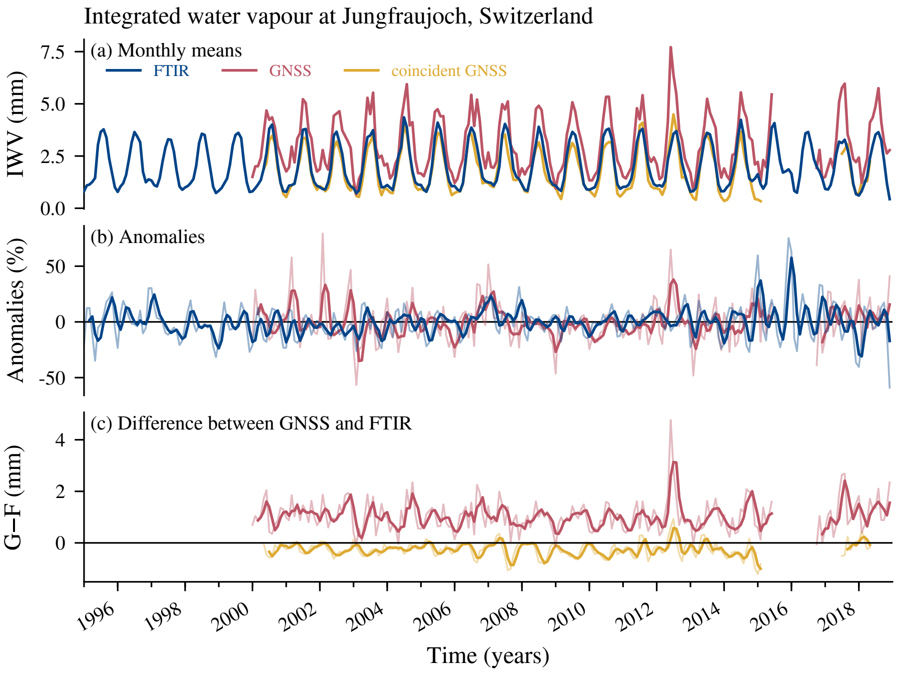

Figure 7. (a) Monthly means of IWV from the FTIR spectrometer and the GNSS station at Jungfraujoch (Switzerland). Shown are GNSS ~~mohthly~~ means once using the full hourly sampling and once using data only at the same time as the FTIR measured (coincident GNSS). The monthly means of FTIR and coincident GNSS have been resampled to correspond to the 15th of each month. **(b)** Anomalies from the climatology ((data−climatology)/climatology) for FTIR data and fully sampled GNSS data. **(c)** Differences between GNSS (G) and FTIR (F) data, using the full GNSS data and GNSS data coincident with the FTIR. The bold lines in **(b)** and **(c)** show the data smoothed with a moving mean window of three months, the thin pale lines show the unsmoothed monthly data.

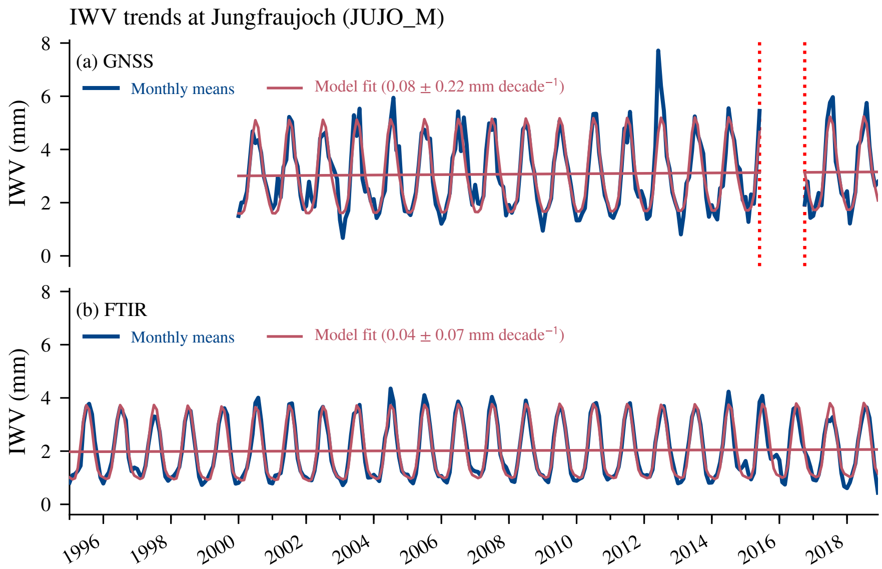

Figure 8. Monthly means and their trend fits for **(a)** GNSS and **(b)** FTIR data at Jungfraujoch. The given trend uncertainty corresponds to $2\,\sigma$ uncertainties. GNSS antenna changes are indicated by vertical red dotted lines.

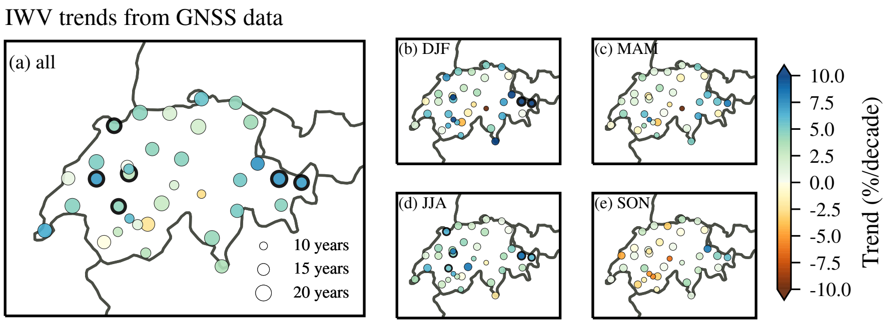

Figure 9. Trends of IWV in Switzerland for the different GNSS stations for **(a)** the whole year~~**(a)** and the four seasons (~~, **(b)** ~~to~~ winter (December, January, February), **(c)** spring (March, April, May), **(d)** summer (June, July, August) and **(e)** autumn (September, October, November). The length of the GNSS time series (Table 1) is indicated by the size of the markers. Stations with trends that are significantly different from zero at 95% confidence interval are marked with a bold edge.

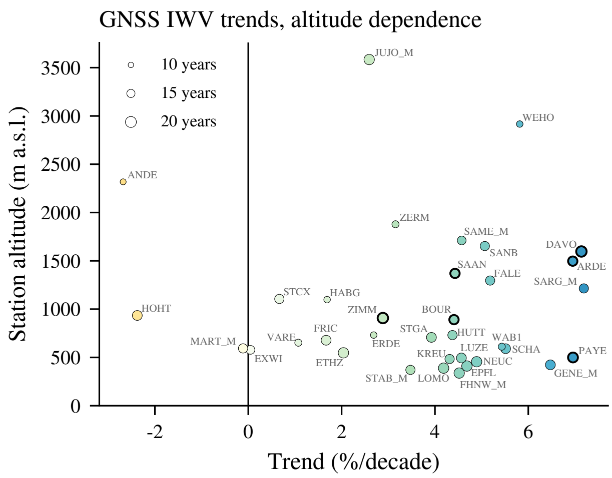

Figure 10. IWV trends from GNSS stations in Switzerland with the station altitude. For merged stations (see Table 1), the averaged altitude of both stations is used. The colors correspond to the trend in percent per decade and are the same as in Fig. 9, the length of the time series is indicated by the size of the markers. Trends that are significantly different from zero are shown with bold edges. The station abbreviations are explained in Table 1.

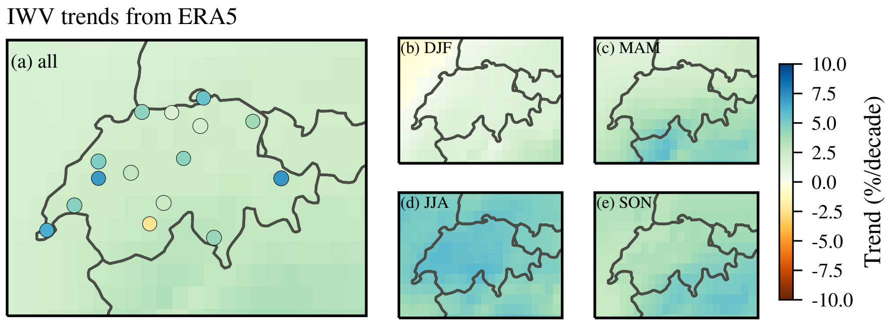

Figure 11. IWV trends from ERA5 reanalysis data in Switzerland from 1995 to 2018 for the whole year **(a)** and for the different seasons (**(b)** to **(e)**). GNSS trends are additionally shown in panel (**a**) (same as in Fig. 9a, but restricted to stations with longest time series of 18 and 19 years).

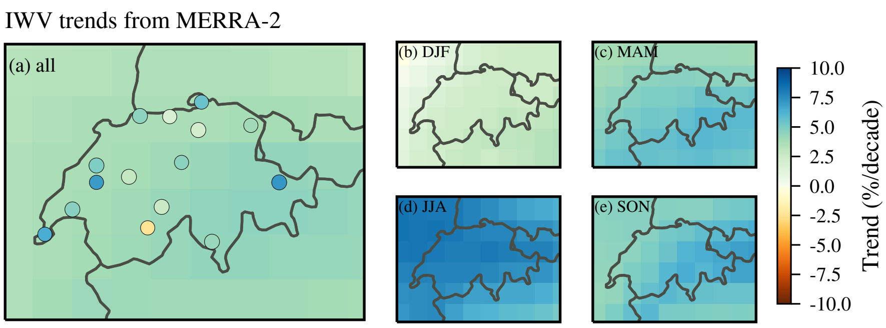

Figure 12. Same as Fig. 11 but for MERRA-2 reanalysis data (1995-2018).

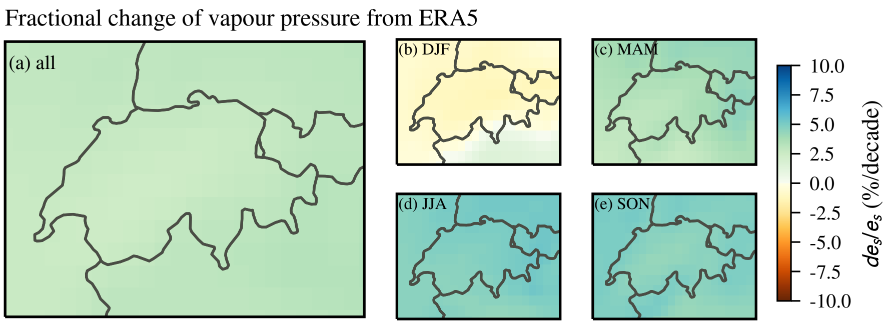

Figure 13. Fractional change of water vapour pressure (e_s) derived from temperature trends from ERA5 (1995-2018) for the whole year **(a)** and different seasons (**(b)** to **(e)**). The temperature data have been averaged below ~~500 hPa~~500 hPa.

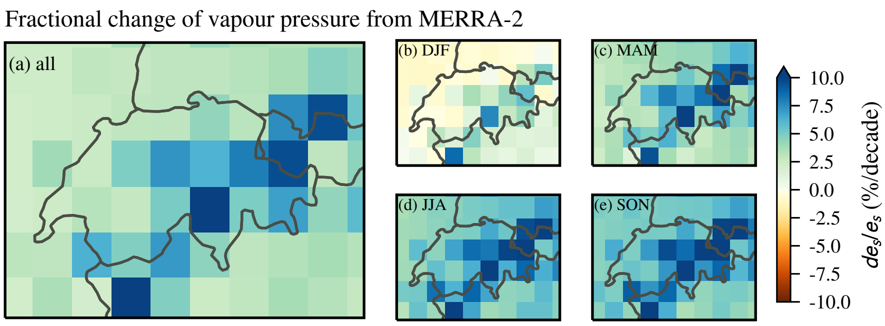

Figure 14. Same as Fig. 13 but using MERRA-2 temperature data averaged below 500 hPa (1995-2018).

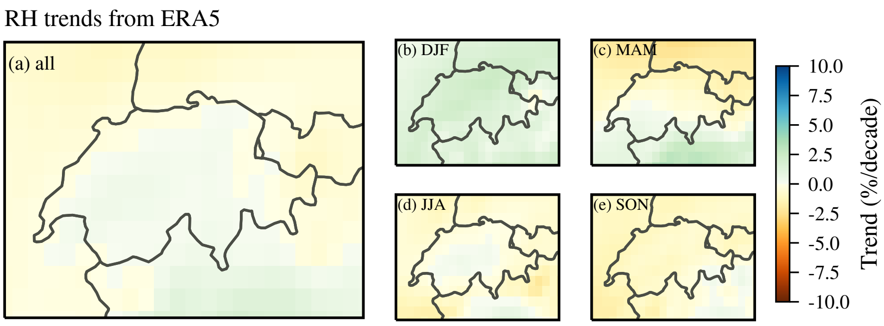

Figure 15. ~~Swiss GNSS stations used~~ Relative humidity (RH) trends from ERA5 reanalysis data in Switzerland from 1995 to 2018 (averaged below 500 hPa) for the ~~present study. Stations marked in bold were directly compared with radiometer~~ whole year **(a)** and ~~reanalysis data at Bern~~ for the different seasons (~~latitutde = 46.95 ± 0.5, longitude = 7.44 ± 1, altitude = 575 ±200 m~~**(b)** to **(e)**).

~~Abbreviation Station name Altitude (m a.s.l.)Data available Remark~~

Table 1. Swiss GNSS stations used in the present study. Stations marked in bold were directly compared with radiometer and reanalysis data at Bern (latitutde = $46.95 \pm 0.5°$, longitude = $7.44 \pm 1°$, altitude = 575 $\pm 200\,\mathrm{m}$).

Abbreviation	Station name	Altitude (m a.s.l.)	Data available	Change points	Remark
ANDE	Andermatt	2318	2000 to 2010	2000-09, 2002-08, 2007-06, 2010-02	
ARDE	Ardez	1497	2002 to 2018		
BOUR	Bourrignon	891	2002 to 2018		
DAVO	Davos	1597	2000 to 2018		
EPFL	EPF Lausanne	411	2000 to 2018	2000-03, 2000-04, 2000-06, 2003-10, 2006-05, 2007-06, 2015-04	
ERDE	Erde	731	2007 to 2018		No AGNES station
ETHZ	ETH Zurich	548	2000 to 2018	2000-03, 2000-08, 2000-09, 2003-05, 2015-05	
EXWI	Exakte Wissenschaften Bern	578	2001 to 2016		No AGNES station
FALE	Falera	1296	2002 to 2018	2007-06, 2010-02	
FHNW_M	Fachhochschule Nordwestschweiz Muttenz	347	2000 to 2018	2007-06, 2015-05, 2018-09	Merged with FHBB (329 m) in 2018
FRIC	Frick	678	2001 to 2018	2008-12, 2015-04	
GENE_M	Geneva	422	2001 to 2018	2007-07, 2009-05, 2015-04	Merged with AIGE (424 m) in 2009
HABG	Hasliberg	1098	2007 to 2018	2007-06, 2010-02	
HOHT	Hohtenn	934	2001 to 2018		
HUTT	Huttwil	731	2002 to 2018	2007-06, 2009-01, 2015-04	
JUJO_M	Jungfraujoch	3584	2000 to 2018	2015-06, 2016-10	Merged with JUJ2 (3585 m) in 2016
KREU	Kreuzlingen	483	2002 to 2018	2006-07, 2006-09, 2007-06, 2015-04	
LOMO	Locarno-Monti	389	2000 to 2018	2007-06, 2015-05	
LUZE	Luzern	494	2001 to 2018	2007-07, 2008-04, 2015-03	

Continued on next page

Continued from previous page

Abbreviation	Station name	Altitude (m a.s.l.)	Data available	Change points	Remark
MART_M	Martigny	594	2002 to 2018	2002-06, 2008-06, 2009-05, 2013-08	Merged with MAR2 (593 m) in 2008
NEUC	Neuchâtel	455	2000 to 2018	2000-09, 2007-06, 2015-04	
PAYE	Payerne	499	2001 to 2018	2000-09, 2007-06, 2015-04	
SAAN	Saanen	1370	2002 to 2018		
SAME_M	Samedan	1709	2003 to 2018	2007-06, 2010-02, 2012-08, 2016-03	Merged with SAM2 (1712 m) in 2016
SANB	San Bernadino	1653	2002 to 2018	2007-06, 2010-02	
SARG_M	Sargans	1211	2002 to 2018	2007-06, 2011-10, 2014-10, 2015-03	Merged with SAR2 (1218 m) in 2011
SCHA	Schaffhausen	590	2001 to 2018	2007-06, 2015-04	
STAB_M	Stabio	371	2002 to 2018	2007-12, 2015-05	Merged with STA2 (371 m) in 2007
STCX	Saint-Croix	1105	2002 to 2018	2007-06, 2010-02, 2013-11	
STGA	St. Gallen	707	2001 to 2018	2007-06, 2007-08, 2015-04	
VARE	Varen	652	2006 to 2018		No AGNES station
WAB1	Wabern	611	2006 to 2018	2005-08, 2009-09, 2016-05	No AGNES station
WEHO	Wetterhorn	2916	2007 to 2018		No AGNES station
ZERM	Zermatt	1879	2006 to 2018	2007-06, 2010-02	
ZIMM	Zimmerwald	908	2000 to 2018		

Table 2. IWV trends for TROWARA in Bern, GNSS stations close to Bern, and reanalysis grids (MERRA-2 and ERA5) at Bern, with $2\,\sigma$ uncertainties. GNSS trends have been bias corrected in case of antenna updates. The uncorrected trends for these stations are given in brackets. Trends that are significantly different from zero at 95 % confidence interval are shown in bold. ~~TROWARA and reanalysis trends are given for the period 1995 to 2018, GNSS trend periods are shown in Table 1.~~

Location	~~Data set~~ **Data set**	~~Trend~~ **Trend** (% per decade)	~~Trend~~ **Trend** (mm per decade)
Bern	TROWARA	**4.8 ± 2.0**	**0.72 ± 0.30**
Bern	~~MERRA2~~ MERRA-2	**3.7 ± 1.7**	**0.53 ± 0.25**
Bern	ERA5	**2.3 ± 1.5**	~~**0.34, ± 0.23**~~ **0.34 ± 0.23**
EPFL	GNSS	~~5.2 ± 5.4~~ 4.7 ± 5.1 **(4.0 ± 2.7)**	~~0.84 ± 0.87~~ 0.75 ± 0.81 **(0.65 ± 0.43)**
EXWI	GNSS	~~0.1 ± 3.9~~ 0.1 ± 4.5	~~0.02 ± 0.60~~ 0.01 ± 0.68
~~Location~~ HUTT	GNSS	~~4.8 ± 6.1~~ 4.4 ± 6.4 (1.0 ± 3.9)	~~0.70 ± 0.88~~ 0.63 ± 0.92 (0.15 ± 0.56)
LUZE	GNSS	~~3.6 ± 5.2~~ 4.6 ± 6.1 (1.6 ± 2.7)	~~0.58 ± 0.84~~ 0.74 ± 0.99 (0.25 ± 0.43)
NEUC	GNSS	~~4.9 ± 5.3~~ 4.9 ± 5.6 (2.1 ± 2.8)	~~0.78 ± 0.84~~ 0.78 ± 0.89 (0.33 ± 0.44)
PAYE	GNSS	~~**7.3 ± 5.3**~~ **7.0 ± 6.3** (2.0 ± 2.9)	~~**1.14 ± 0.93**~~ **1.09 ± 0.98** (0.32 ± 0.46)
WAB1	GNSS	~~5.5 ± 8.0~~ 5.4 ± 8.2 (3.4 ± 3.9)	~~0.95 ± 1.39~~ 0.94 ± 1.41 (0.59 ± 0.68)